AN ABSTRACT OF THE THESIS OF

Thomas David Roberts (Name) for the Ph. D. (Degree) in Physics (Major)

Date thesis is presented April 7, 1965

Title EXPERIMENTAL DETERMINATIONS OF ELECTRON ENERGY DISTRIBUTIONS FOR TOWNSEND DISCHARGES IN HELIUM GAS.

Abstract approved Redacted for Privacy
(Major professor)

The energy distribution of electrons in Townsend discharges in helium has been experimentally investigated in a direct fashion.

A discharge is initiated between parallel plates of a small cell mounted at the center of a spherical retarding field energy analyzer. The anode of the cell is perforated and some electrons from the discharge enter the retarding field region. Pressures in the discharge cell are of the order of 1 torr and the pressure in the analyzer region is about $10^{-7}$ torr, so no significant alteration of the electron energy spectrum due to collisions takes place after electrons have left the discharge cell. The electron current reaching the collecting surface of the analyzer is measured as a function of retarding field strength. The usual perturbations due to probe measurements in the discharge itself are thus minimized.

The interaction of electrons with the surfaces of the analyzer is considered, and the experimental data are corrected for the

resulting electron reflection and secondary emission. A gold black analyzer surface exhibiting low total electron secondary emission coefficient is utilized.

Experimental electron energy distributions are compared with the theoretical calculations of Heylen and Lewis, and qualitative agreement is found for helium. The correction due to electron reflection and secondary emission is shown to be minor.

# EXPERIMENTAL DETERMINATIONS OF ELECTRON ENERGY DISTRIBUTIONS FOR TOWNSEND DISCHARGES IN HELIUM GAS

by

THOMAS DAVID ROBERTS

A THESIS

submitted to

OREGON STATE UNIVERSITY

in partial fulfillment of
the requirements for the
degree of

DOCTOR OF PHILOSOPHY

June 1965

APPROVED:

Redacted for Privacy

Associate Professor of Physics

In Charge of Major

Redacted for Privacy

Chairman of Department of Physics

Redacted for Privacy

Dean of Graduate School

Date thesis is presented April 7, 1965

Typed by Marion F. Palmateer

## ACKNOWLEDGMENTS

I am indebted to Dr. David S. Burch, my major professor, for his guidance throughout the course of this study, and for the original idea of the experiment.

I should also like to express my gratitude to Ralph C. Applebee for his unsolicited help with problems which arose, both in and out of the laboratory, during the years required to bring this work to completion.

TABLE OF CONTENTS

LIST OF FIGURES

# EXPERIMENTAL DETERMINATIONS OF ELECTRON ENERGY DISTRIBUTIONS FOR TOWNSEND DISCHARGES IN HELIUM GAS

## INTRODUCTION

The nature of the energy distribution of electrons in a non-self-sustained gas dischage has been the subject of extensive theoretical investigations, the results of which have heretofore not been verified experimentally in any direct way. This report describes such direct measurements of the energy distribution exhibited by electrons in a Townsend discharge in helium gas at intermediate values of $\frac{E}{p}$.

The distribution of velocities among a large number of molecules situated in a volume element of real space* $d\underline{r}$ is customarily expressed in terms of a so-called velocity distribution function $f(\underline{c}, \underline{r}, t)$ (3, p. 27). This function is defined in such a way that the quantity

$$f(\underline{c}, \underline{r}, t)\, d\underline{c}\, d\underline{r}$$

represents the probable number of particles which are in the volume element $d\underline{r}$ containing $\underline{r}$ and which have velocities in a range $d\underline{c}$ about

---

*Here the notation convention followed by Chapman and Cowling (3) is used, namely, that the symbol $d\underline{r}$ represents an element of volume enclosing the terminus point (x, y, z) of the vector $\underline{r}$. Thus, in Cartesian coordinates, for example, $d\underline{r}$ is taken as the parallelepiped dxdydz. Similar remarks apply to the volume element in velocity space $d\underline{c}$.

the value $\underline{c}$ at time t. The probable number of molecules $nd\underline{r}$ in the volume element $d\underline{r}$ is found by integrating $fd\underline{c}d\underline{r}$ over all velocity space, so the number density n is simply

$$n = \int f(\underline{c}, \underline{r}, t)dc \,. \tag{1-1}$$

From the above comments, one sees that the function f can be regarded as a number density of points in the six-dimensional velocity-position space formed by the coordinates of $\underline{c}$ and $\underline{r}$, and that the definition of f is based on the statistical behavior of the gas. Mean values of functions of molecular (or particle) velocities are obtained from the expression

$$\langle g \rangle = \frac{\int g f d\underline{c}}{\int f d\underline{c}} \,, \tag{1-2}$$

where $g(\underline{c})$ is any function of the particle velocity $\underline{c}$, and the integration is over all velocity space. One important function of this type is the particle velocity itself, $\underline{c}$, and the mean value of the this quantity is clearly

$$\langle \underline{c} \rangle = \frac{\int c f d\underline{c}}{\int f d\underline{c}} \,. \tag{1-3}$$

Although originally used to describe the behavior of colliding hard spheres with no force of attraction or repulsion between them, the

same definitions and statements are applied when electrons in dilute gases are considered; one merely substitutes the word "electron" wherever the word "molecule" or "particle" appears. The function f thus becomes the electron velocity distribution function, and $\langle \underline{c} \rangle$ the mean electronic velocity.

If a uniform electric field is applied to a mixture of electrons and gas molecules, the motion of electrons colliding with the molecules and each other can be described by a net macroscopic "drift" velocity antiparallel to the field direction. This drift velocity $\langle \underline{c} \rangle$ is obtained from an expression similar to 1-3 and is of considerable interest in the study of electrons in gases, because it may be readily measured. Another quantity of interest which is closely related to the drift velocity is the ratio of the drift velocity to the applied electric field, the so-called "mobility". In general, calculations of such quantities and any other parameters describing the probable, or average, behavior of electrons implies knowledge of the distribution function for electronic velocities under specified conditions.

In 1913, Townsend performed experiments dealing with the mobilities of electrons in gases which indicated electrons in an electric field in a gas have a higher average energy than the surrounding gas molecules (37). This discovery prompted theoretical derivations of the distribution law obeyed by electrons in a field in a gas. Early derivations resulted in the well-known Maxwellian law. The usual

form of Maxwell's velocity distribution function is (3, p. 72)

$$f = n\left(\frac{m}{2\pi kT}\right)^{3/2} e^{-\frac{mc^2}{2kT}} \quad . \tag{1-4}$$

or, expressed as a distribution of speeds, where $f\underline{dc} = f_s dc$,

$$f_s = \left(\frac{2}{\pi}\right)^{\frac{1}{2}} n \left(\frac{m}{kT}\right)^{3/2} c^2 e^{-\frac{mc^2}{2kT}} \quad . \tag{1-5}$$

In terms of electron energies*, we have

$$f_\epsilon = \left(\frac{2}{\pi}\right)^{\frac{1}{2}} n \left(\frac{m}{kT}\right)^{3/2} \epsilon^{\frac{1}{2}} e^{-\frac{\epsilon}{kT}} \quad , \tag{1-6}$$

where $\epsilon = \frac{1}{2}mc^2$. Here m is the molecular mass, T is the absolute gas temperature and k is the Boltzmann constant.

As the atomic theory became more completely developed, other derivations of the electron energy distribution function were carried out. In 1930, M. J. Druyvesteyn (7) succeeded in obtaining a distribution law which was rederived from a different approach by Morse, Allis and Lamar in 1935 (26). Both derivations were subject to the following conditions:

1. The collision frequency for electron-electron interactions

---

*Henceforth, this paper will consider energy distribution functions, rather than speed or velocity distributions unless otherwise noted.

is negligible compared to the collision frequency for electron-molecule collisions; i. e.,

$$\nu_{e-e} \ll \nu_{e-m} .$$

2. Only elastic interactions occur.

3. Electrons lose some energy upon impact with the gas molecules, as required by momentum conservation.

When a constant diffusion cross section was assumed for electron-molecule interactions, it was found that f assumes the form

$$f = K_1(\epsilon)\, e^{-\frac{\epsilon^2}{2\epsilon_o}} . \qquad (1-7)$$

The principal difference between this function, termed the Druyvesteyn distribution, and the Maxwellian function is the appearance of $\epsilon^2$ in the exponent, rather than $\epsilon$. Later theoretical approaches yielded the same form as Druyvesteyn's result, when the same limiting conditions were imposed.

In 1960, Dreicer (5) predicted that as the electron density becomes sufficiently large that electron-electron collisions have an important effect, the electron energy distribution makes a smooth transition from Druyvesteyn to Maxwellian form. For large electron densities in highly ionized gases, or "plasmas", probe techniques have indicated that the electron energy distribution is indeed Maxwellian

(17). Dreicer's derivation included the effects of both Coulomb and electron-neutral collisions in the transition region between poorly ionized and highly ionized gases.

Earlier, about 1958, T. J. Lewis had initiated a theoretical study of the electron energy distribution in this transition region using a somewhat different point of view. The culmination of his effort appeared as a paper which was written jointly with A. E. D. Heylen (13) in which Coulomb interactions were ignored (implying low electron densities), and use was made of the experimental form of the total inelastic and elastic scattering cross sections for electron-helium interactions. The result of this analysis is of considerable interest, because the distribution function has a form which is quite decidedly neither Druyvesteyn nor Maxwellian in the transition region. Parameters such as diffusion coefficients, electron mobilities, mean energies and ionization coefficients calculated using the distribution are in agreement with experiment, where such experiments have been performed.

At the onset of the experiment described herein, the nature of the energy distribution in the transition regime of intermediate values of $\frac{E}{p}$ was not well understood, either qualitatively or quantitatively. Such knowledge is essential to an understanding of the macroscopic parameters usually employed to describe the behavior of electrons in gases, even if the knowledge is only of a qualitative nature.

# THEORETICAL DISCUSSION

## The Boltzmann Transport Equation

The traditional formal approach to the theoretical problem of finding the distribution function for any given system is to solve the equation of motion for the distribution function. This equation is readily obtained in its general form by considering first the case where molecules do not interact, in which case molecules contained in a six-dimensional space element $d\underline{r}d\underline{c}$ at $(\underline{r}, \underline{c})$ are in an element $d\underline{r}'d\underline{c}'$ at $(\underline{r} + \underline{c}\delta t, \ \underline{c} + \frac{\underline{F}}{m}\delta t)$ after the time interval $\delta t$. Here $\frac{\underline{F}}{m}$ is the acceleration of a particle due to external forces applied to the gas, and $m$ is the mass of one such particle. Ascribing the alteration in $f$ during $\delta t$, $f(t + \delta t) - f(t)$, to the effect of collisions, one obtains (after expansion to the first order of $\delta t$) the well-known equation (5):

$$\left(\frac{\partial}{\partial t} + \underline{c} \cdot \nabla_{\underline{r}} + \frac{\underline{F}}{m} \cdot \nabla_{c}\right) f(\underline{r}, \underline{c}, t) = \left(\frac{\partial f}{\partial t}\right)_{coll} \qquad 2\text{-}1$$

Substitution of an explicit form for the term $\left(\frac{\partial f}{\partial t}\right)_{coll}$ yields an integro-differential equation which describes the development of the distribution function $f$ with time. In particular, it is possible, under certain restrictive assumptions (16, p. 65-67), to obtain a slightly less general form of Equation (2-1), the Boltzmann transport equation:

$$\left(\frac{\partial}{\partial t} + \underline{c}_1 \cdot \nabla_{\underline{r}} + \frac{\underline{F}}{m} \cdot \nabla_{\underline{c}}\right) f_1 = \int d\Omega \int d^3\underline{c}_2 \sigma(\Omega)\left(|\underline{c}_2 - \underline{c}_1|\right)\left(f_2' f_1' - f_2 f_1\right), \quad (2\text{-}2)$$

where the velocities of the two particles interacting before the collision are $\underline{c}_1$ and $\underline{c}_2$ and the velocities after the binary interaction are $c_1'$ and $c_2'$, $f_1 = f(\underline{r}, \underline{c}_1, t)$, $f_2 = f(\underline{r}, \underline{c}_2, t)$, $d\Omega$ is the differential of solid angle, and $\sigma(\Omega)$ is the differential cross section.

The Theory of Heylen and Lewis

Although the usual procedure for obtaining a distribution function for a given system is to solve Equation (2-2), Heylen and Lewis have chosen a slightly different approach and have considered the so-called Smit equation for electrons in a uniform field which may be written (34)

$$\Sigma\left[n_1(\epsilon) - n_2(\epsilon)\right] = 0 .$$

This equation is a mathematical statement of the assumption that for a steady state condition, $\Sigma n_1(\epsilon)_1$, the number of electrons per second in a given volume element in six-space moving upward in energy and passing through the energy $\epsilon$ due to all interactions is equal to $\Sigma n_2(\epsilon)$, the number moving down. The summation is over all processes by which electrons can gain or lose energy.

After considerable manipulation, it is possible to write

Equation (2-3) as

$$\left[2\frac{m}{M}N\theta_d\epsilon^{3/2} - \frac{1}{6}\frac{\epsilon^2}{N\theta_d}\epsilon^{-\frac{1}{2}}\right] g(\epsilon) + \frac{E^2}{3N\theta_d}\epsilon^{\frac{1}{2}}g(\epsilon) + N\Sigma_j \int \epsilon^{\frac{1}{2}} Q_j(\epsilon) g(\epsilon)\, d\epsilon = 0, \quad (2\text{-}4)$$

which is subject to the assumption that the electrons have much greater energies than the mean gas energy. Here, $\frac{m}{M}$ is the electron/molecule mass ratio, $\theta_d$ is the diffusion cross section, $Q_j(\epsilon)$ is the cross section of an inelastic collision with onset energy $\epsilon_j$, $N$ is the number of gas molecules per unit volume, $\epsilon$ is the electronic energy, and $g(\epsilon)$ is the energy distribution function, now assumed to be independent of the spatial coordinates, where $g(\epsilon) = \epsilon^{\frac{1}{2}} f(\epsilon)$.

Differentiating Equation (2-4) with respect to $\epsilon$, one finds

$$g'' + (b-q)g' + \left(\frac{1}{4\epsilon^2} + \frac{q}{2\epsilon} + \frac{b}{\epsilon} + \frac{b'}{2}\right)g + \frac{3N^2\theta_d}{E^2}\epsilon^{-\frac{1}{2}} \sum_j \left[(\epsilon+\epsilon_j)^{\frac{1}{2}} Q_j(\epsilon+\epsilon_j) g(\epsilon+\epsilon_j) - \epsilon^{\frac{1}{2}} Q_j(\epsilon) g(\epsilon)\right] = 0. \quad (2\text{-}5)$$

where

$$b = \frac{6m}{M}\left(\frac{N\theta_d}{E}\right)^2\epsilon \quad \text{and} \quad q = \theta_d^{-1}\frac{d}{d\epsilon}\theta_d \quad (2\text{-}6)$$

This equation, which is a differentiated form of the Smit equation, can be obtained directly by manipulation of the Boltzmann equation. The development is quite lengthy; many of the essentials are contained in

a paper by Holstein (15). The main point is that the two approaches merge at this equation; that is, Equation (2-5) may be obtained from either the Smit equation or the Boltzmann equation. Heylen and Lewis employed the following assumptions in solving the restricted problem for electrons in monatomic gases:

1. Since optical excitation collisions occur for relatively large $\epsilon_j$, it is assumed that $g(\epsilon + \epsilon_j) << g(\epsilon)$. The authors suggest that the assumption is good unless $\epsilon < 1$ eV. The summation term in Equation (2-5) thus becomes $-\epsilon^{\frac{1}{2}} g(\epsilon) \Sigma_j Q_j(\epsilon)$.
2. The sum of all inelastic cross sections is replaced by a total inelastic cross section $Q(\epsilon) = \Sigma_j Q_j(\epsilon)$.
3. The momentum transfer cross section $\theta_d$ is replaced by the total elastic cross section $\theta$.
4. The function $N\theta$ is approximated by the function $N\theta = 26 \exp(-.04\epsilon)$, where $\epsilon$ is in electron volts.

These assumptions, coupled with a procedure originally due to Langer (19), are employed to obtain a functional form of the energy distribution. The development is quite involved; the result may be expressed in the form

$$g(\epsilon) = k\left[\frac{N\theta}{(\frac{1}{4}\beta^2+\frac{1}{2}\frac{\beta}{E}+\frac{3(N\theta)(NQ)}{E^2})^{\frac{1}{2}}}\right]^{\frac{1}{2}}\exp\left\{-\int_o^{\epsilon}(\tfrac{1}{4}\beta^2+\tfrac{1}{2}\frac{\beta}{E}+\frac{3(N\theta)(NQ)}{E^2})^{\frac{1}{2}}d\epsilon\right\} \quad (2\text{-}7)$$

for helium. Here k is a normalizing constant; $\beta$ is a constant whose numerical value is given by Heylen and Lewis as 0.04 when all energies are expressed in electron volts. The total inelastic cross section Q is zero below the first excitation potential for helium; it rises with increasing energy for energies above this first excitation level. The result of calculations using Equation (2-7) are shown in Figure 1. Note the sharp curtailment of $g(\epsilon)$ at the onset potential $\epsilon_e$. This sharp change in slope at the onset potential is in contrast to results obtained by others (5), and this is a distinguishing feature of Heylen and Lewis' work. At high values of $\frac{E}{p}$,

$$\tfrac{1}{4}\beta^2+\tfrac{1}{2}\frac{\beta}{E} \gg \frac{3(N\theta)(NQ)}{E^2}, \quad (2\text{-}8)$$

so that $g(\epsilon)$ tends to a limiting form governed by $\beta$ which is nearly Maxwellian. At very low $\frac{E}{p}$, in particular $\frac{E}{p} = 5$, the results are in fair agreement with results obtained by Smit and Barbiere. Thus, at low or high $\frac{E}{p}$, the theoretical results fall roughly in line with the results of previous investigations; it is only in the region of intermediate $\frac{E}{p}$ that the distribution behaves in a manner other than one might deduce from previous derivations. The units of $\frac{E}{p}$ throughout

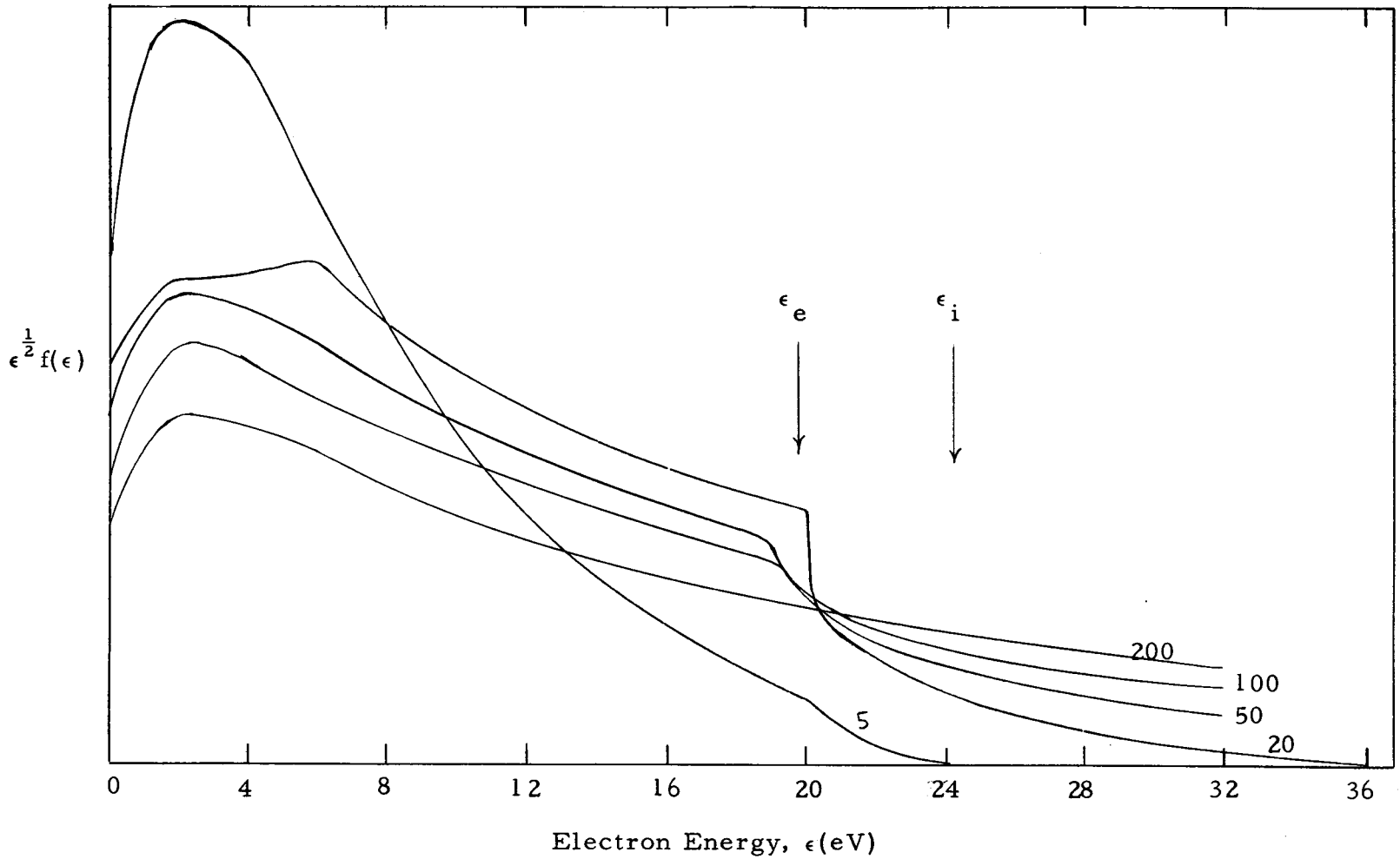


Figure 1. Electron Energy Distributions for Helium at Various Values of $\frac{E}{p}$ as calculated by Heylen and Lewis.

the paper are volts/cm torr, in accordance with conventional practice.

Assumption 1, above, casts some doubt on the validity of Heylen and Lewis' results for low values of the energy $\epsilon$. Depending on the exact position of the maximum of the actual distribution obeyed by electrons in a discharge, and the magnitude of the change in slope at the onset potential, the number $g(\epsilon + \epsilon_j)$ could be quite comparable to $g(\epsilon)$. This leaves the actual shape of the distribution function $g$ for low electron energies open to speculation.

# EXPERIMENTAL DESIGN CONSIDERATIONS

This discussion of the experimental design considerations is divided into four parts: the experimental method, the simple theory of retarding field energy analysis, a consideration of energy resolution restrictions for spherical geometries, and the effect of selective reflection and secondary emission of electrons from collecting surfaces.

## The Experimental Method

The use of a current probe located between the parallel plates of a gas discharge tube represents a traditional approach to the problem of obtaining the energy distribution of electrons in an ionized gas. The introduction of a probe into the discharge region can be tolerated in the case of a highly ionized gas with high electron densities (20, p. 330). In such cases, it is assumed that the presence of a high-resistance probe does not perturb the discharge to a degree sufficient to alter the electron energy distribution appreciably, largely because of the presence of a positive ion space charge sheath between the metal of the probe and the gas. The introduction of a probe in a weakly ionized gas (a Townsend discharge, for example) raises the possibility of extensive field distortion and subsequent alteration of the electron energy spectrum. If the energies of electrons in a Townsend discharge are to be experimentally observed, one must

devise a scheme other than the use of probes.

A simplified schematic of the method employed in this experiment is shown in Figure 2. Electrons emitted from the cathode drift toward the anode of the central cell under the influence of a uniform electric field, making collisions with gas atoms. After proceeding some distance $d_o$ from the cathode, the electrons achieve an equilibrium energy distribution which is maintained throughout the region $(d - d_o)$. All the electrons are collected at the anode, save for those escaping by effusive flow through the perforation located in the center of the anode. The region exterior to the cell is at a pressure much lower than the pressure inside, and electrons which escape through the hole ideally make no collisions once outside, so no further alteration of the equilibrium energy distribution occurs, except for possible weighting of the distribution by a velocity factor. This weighting effect is to be discussed in subsequent sections. An electric field is maintained between the spherical conductor which serves as a collector for the electrons and the anode. The direction of the field is such as to retard the flow of electrons; to be collected, electrons must have sufficient initial energy to overcome the field. By increasing or decreasing the intensity of the retarding field and observing the effect on the collected current, one obtains data which may be related to the energy distribution.

The method outlined above has several apparent advantages.

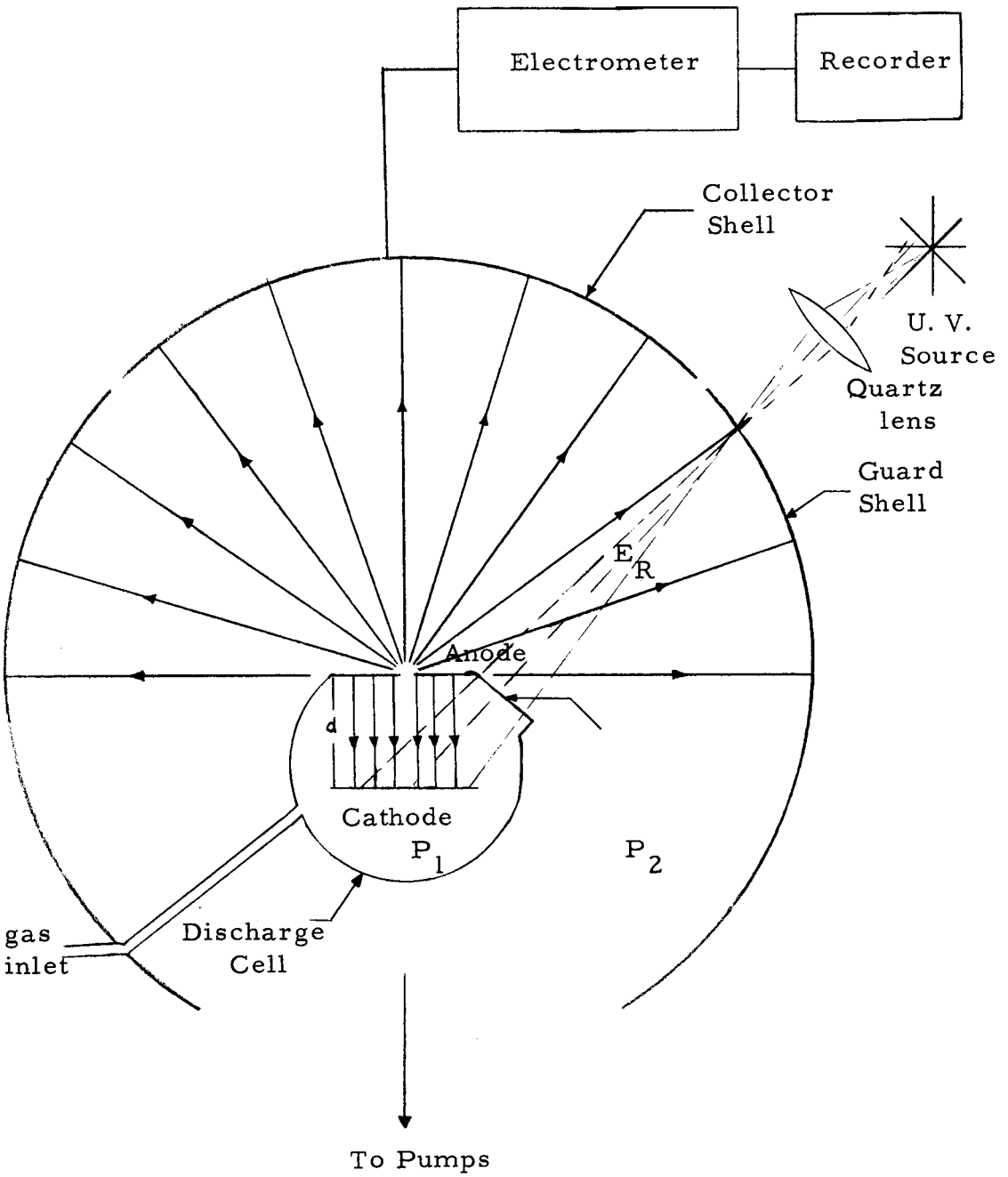


Figure 2. Simplified Schematic of Energy Distribution Experiment.

The retarding field is applied in a region remote from the discharge itself, thus circumventing the possibility of distorting the uniform field, except for the region in the immediate vicinity of the hole. The retarding field is nearly radial, so escaping electrons travel parallel to field lines over most of their trajectories, which would not be the case for, say, a plane collecting surface. The spherical geometry also permits relatively simple calculations to be performed when factors such as energy resolution and electron reflection are studied.

## Simple Theory of Retarding Field Energy Analysis

If a point source of electrons is located at the center of a hollow spherical conducting shell, as is the case for an infinitesimal discharge cell, it is possible to obtain the distribution of electronic energies of the source by varying the electric potential between the source and the conducting shell, while simultaneously measuring the electron current as a function of applied potential. If the energy spectrum of the source is such that electrons have energies ranging from zero electron volts to some maximum value, say $V_m$ electron volts, the potential applied to the conducting sphere relative to the source must range between zero volts and $-V_m$ volts. At an applied potential difference of slightly less than $-V_m$ volts, no electrons reach the spherical surface save the most energetic ones. Conversely, at zero volts potential difference, all electrons emitted from the source have

sufficient energy to reach the conducting surface; if there is no reflection of electrons from the surface, all are collected, and all of the electrons from the source contribute to the current i. If the potential difference between the conducting sphere and source is $-V'$ volts, where $0 < V' < V_m$, only those electrons with initial energies greater than $V'$ electron volts have sufficient energy to overcome the potential "hill" between source and collecting sphere, and each falls incident on the conducting surface with energy $V'' - V'$, where $V''$ is the initial energy of the electron under consideration. The situation for an arbitrary distribution is shown in Figure 3. The total number of electrons collected is proportional to the area under the distribution curve to the right of $V'$, with a resulting current

$$i(V') = A\int_{eV'}^{eV_{max}} \epsilon^{\frac{1}{2}} g(\epsilon) d\epsilon \,. \qquad (3\text{-}1)$$

Thus, the integral of the distribution, a function of the lower limit $eV'$, is directly related to the function one obtains upon plotting the current $i(V')$ as a function of $V'$.

The exact relation between $i(V')$ and the energy distribution function in this simple analysis can be found from the relation

$$dj(c) = (dn)\, ec \,, \qquad (3\text{-}2)$$

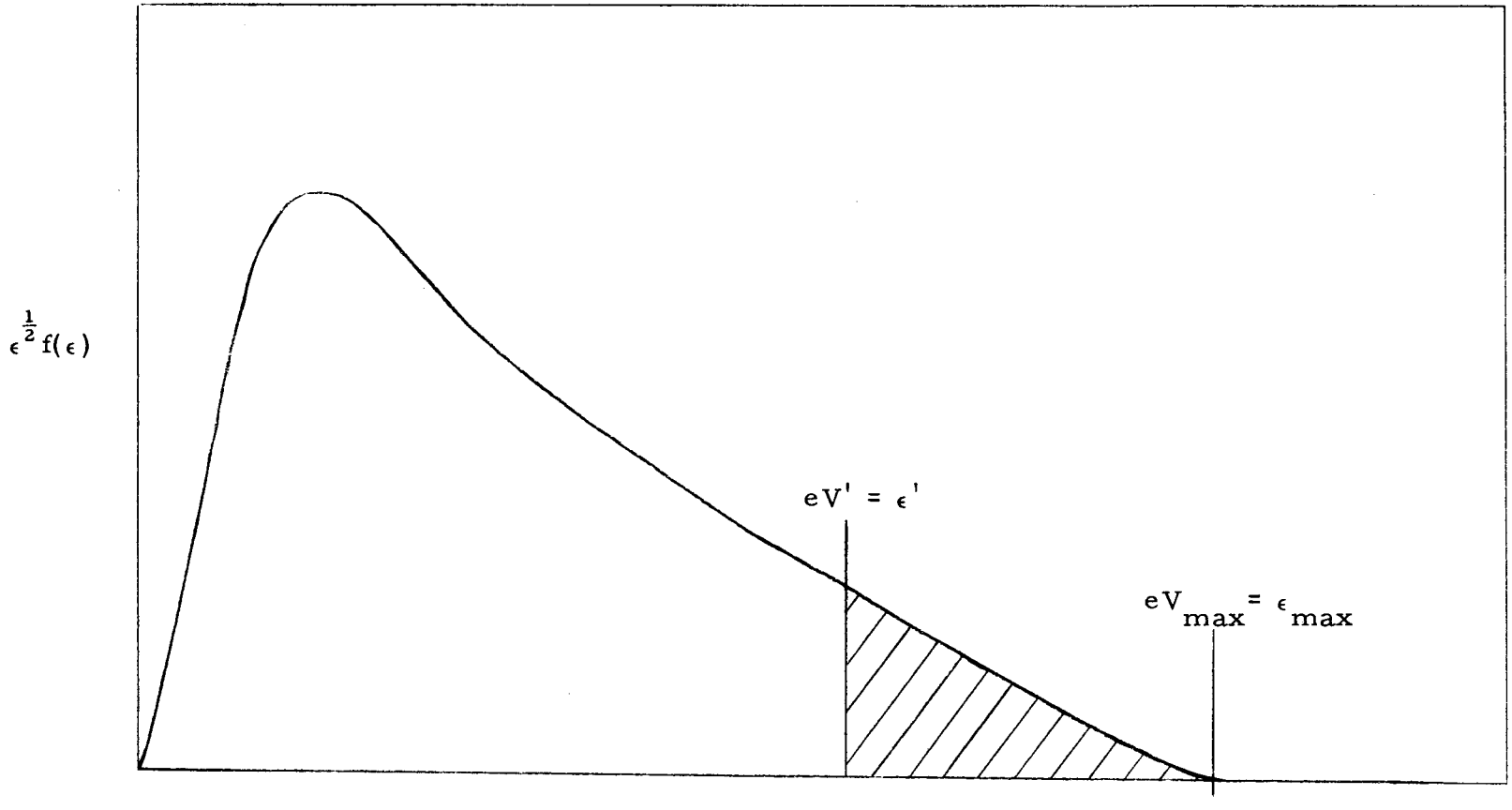


Figure 3. Hypothetical Electron Energy Distribution.

where dj(c) is the current density due to electrons moving with a range of velocities dc about the value c along any radial path of infinitesimal cross-sectional area, dn is the number density of electrons having speed in a range dc about c at the spherical surface*, and e is the electronic charge. From Equation 1-1,

$$dj(c) = f(c)ec^3(dc) \tag{3-3}$$

Hence,

$$\frac{dj}{dc} = fec^3 \tag{3-4}$$

At any value of repelling potential $V'$, for an electron with initial energy $eV > eV'$, the final energy is related to the speed by

$$\tfrac{1}{2}mc^2 = e(V - V') \tag{3-5}$$

and

$$mc(dc) = -edV' . \tag{3-6}$$

Thus,

$$\frac{dj}{dc} = \frac{dj}{dV'}\frac{dV'}{dc} = \frac{-mc}{e}\frac{dj}{dV'} . \tag{3-7}$$

Making use of this result in Equation (3-4), we have

$$\frac{dj}{dV'} = \frac{-e^2}{m} fc^2. \tag{3-8}$$

*It is assumed that the source emits isotropically, to eliminate geometric constants.

The course of an experiment to determine the energy distribution of electrons of the source is, then, to obtain magnitudes of the collected current for different values of the applied retarding potential and then differentiate the resulting curve to obtain f.

If the point source of electrons is replaced by a discharge cell such as the one described above but of infinitesimal size, the result given by Equation (2-9) is directly applicable to the problem of finding the energy distribution of electrons in a Townsend discharge. That the experiment cannot be so idealized, however, is made clear in the following sections of this chapter.

## Energy Resolution

If the source of electrons at the center of the spherical shell in Figure 2 is other than a point source, a finite limit is placed on the energy resolution of the analyzer, because electrons no longer travel parallel to electric field lines. Simpson (32) points out that when electron trajectories cross field lines, some electrons which have enough energy to overcome the potential hill between the source and the collector never reach the collector plate, and an uncertainty in the energy, $\Delta\epsilon$, is introduced into the experiment. The failure to collect such electrons comes about because only that component of the electron's momentum perpendicular to equipotential lines is decreased under the action of the retarding field; the parallel component

is unchanged in magnitude. Of course, for a point source of electrons this never occurs, and the resolution of the idealized set-up discussed in the previous section is infinite. This is not the case for the actual experimental configuration. The field-line pattern for the disc-sphere configuration used in this experiment, Figure 4, is obtained from a solution of the problem of finding the potential at any point due to a circular disc of radius $a$ at a potential $V_1$ given by the expression (35, p. 206)

$$V = \frac{2V_1}{\pi} \sum_n (-1)^n (2n+1)^{-1} \left(\frac{a}{R}\right)^{2n+1} P_{2n}(\cos\theta), \quad 0 \leqslant n < \infty \ . \qquad (3\text{-}9)$$

The equation for the electric field is obtained from $\underline{E} = -\nabla V$. One finds, retaining terms upto $\left(\frac{a}{R}\right)^3$ only,

$$E_r = \frac{2V_1}{\pi} \frac{a}{R^2} \left[1 - \tfrac{1}{2}\left(\frac{a}{R}\right)^2 (3\cos^2\theta - 1)\right]; \qquad (3\text{-}10)$$

$$\frac{\pi}{2V_1} E_\theta = -\frac{a^3}{R^4} \sin\theta \cos\theta .$$

Two features are apparent from examination of Figure 5:

1. Electrons emitted from the vicinity of the disc travel parallel to field lines for a greater portion of their trajectory for larger values of the ratio $\frac{R}{a}$ .
2. Electrons travelling to the central section of the sphere,

$$\kappa \underline{E} = \hat{r}\,\frac{1}{R^2}\left[1 - \frac{a^2}{2R^2}(3\cos^2\theta - 1)\right] - \hat{\theta}\,\frac{a^2}{R^4}\cos\theta\,\sin\theta$$

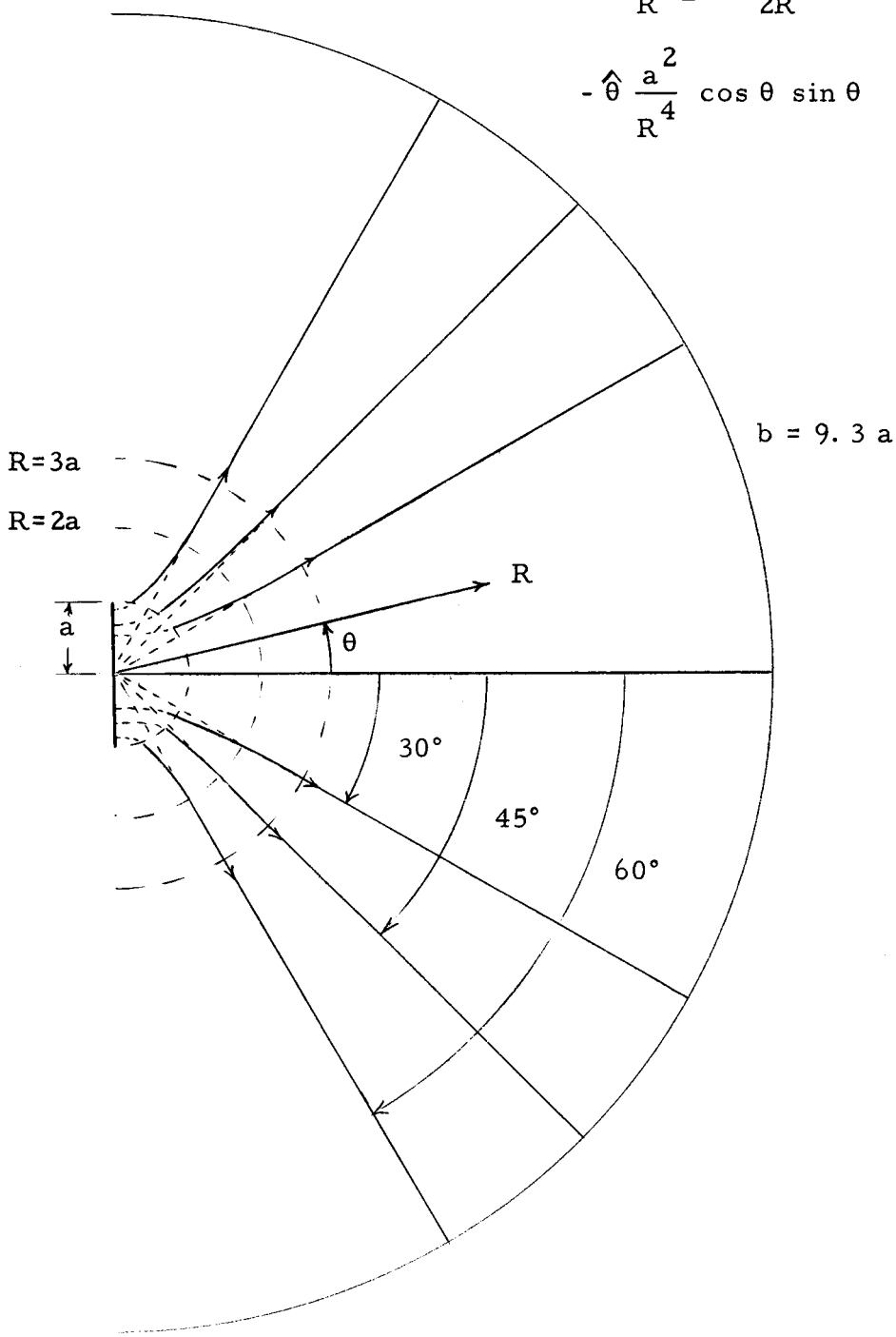


Figure 4. Electric Field Lines for Central Disc of Radius a.

i. e., at smaller angles $\theta$, have trajectories more nearly parallel to field lines.

Hence, it is desirable to make the ratio $\frac{R}{a}$ as large as possible and to use as small a central region of the sphere as a collector as is practical, the remainder of the sphere serving as a guard shell at the same potential to prevent edge effects.

The fractional spread in the energy $\epsilon$ of electrons which are collected for any given field intensity is represented by the quantity $\frac{\Delta \epsilon}{\epsilon}$. Lukirsky (21) has shown that for concentric spheres of radii a and b, $a < b$, this uncertainty depends on the square of the ratio of the radii and the angle at which electrons emerge from a hole in the central sphere;

$$\frac{\Delta \epsilon}{\epsilon} = \left(\frac{a}{b}\right)^2 \sin^2\theta \ . \qquad (3\text{-}11)$$

This result is obtained by solving the central force problem of finding the orbit of a charged particle in the region between the spheres and examining the case for which an elliptical trajectory just grazing the collector is followed.

The situation is complicated somewhat when the inner sphere is replaced by a disc, as in this experiment, but the problem has been solved numerically by Soboleva (36), who indicates the result is not much different than for concentric spheres, so long as the electrons

are emitted from the center of the disc.

From the foregoing discussion it is clear that any alteration of the electron trajectory from one parallel to field lines is detrimental to the inherent resolution of a retarding field analyzer. Consequently, the effect of the component of the geomagnetic field perpendicular to the electron path must be taken into account, particularly when considering slow electrons. One way of reducing its undesirable effect is by shielding the apparatus from the magnetic field as much as possible. Another method for minimizing the effect is to decrease the ratio $\frac{b}{a}$, but this is undesirable, as seen from Equation (3-11). The procedure followed in this experiment was to shield the analyzer as much as possible, while keeping the ratio $\frac{b}{a}$ fairly large.

## Electron Reflection

When electrons fall incident on a metallic surface, some of them are not collected, but are reflected elastically. These, together with electrons released by secondary emission, constitute a current in a direction opposite to the incident current. The magnitude of this current is a function of the energy of the incident electrons (9), which generally increases with increasing energy up to 50 eV or more. If a repelling potential gradient exists between a central electron source and a collecting sphere, some electrons which have enough energy to overcome the potential hill are not collected, but rather are reflected

elastically or give rise to secondary electrons. Recognition of this phenomenon requires some modification of the simple theory of the spherical energy analyzer.

If an electron gun is mounted in the center of the sphere, and the region between the electron gun and the conducting surface is field-free (Figure 5), a measure of the amount of reflection and secondary emission is obtained by directing a thin, monoenergetic electron beam at the top collecting portion of the sphere only. If the beam is sufficiently well-focused, no primary current is incident on the remainder of the sphere, and a galvanometer placed in the guard shield circuit reads only the reflected current. Further, if it is assumed that multiple reflections from the guard shield resulting in some electrons being returned to the collector are unimportant, a ratio between primary and total current may be formed at any given beam energy. This ratio is the fractional current which is collected at a given energy and is

$\frac{i_c(\epsilon)}{(i_c(\epsilon) + i_g(\epsilon))} = T(\epsilon)$, where $i_c$ is the current in the collector circuit,

and $i_g$ is the current measured in the guard shield circuit. In an experiment of this kind, one frequently defines a quantity called the total secondary emission coefficient, $\delta$, given by (18)

$$\delta(\epsilon) = 1 - T(\epsilon) = \frac{i_g(\epsilon)}{i_c(\epsilon) + i_g(\epsilon)}. \qquad (3\text{-}12)$$

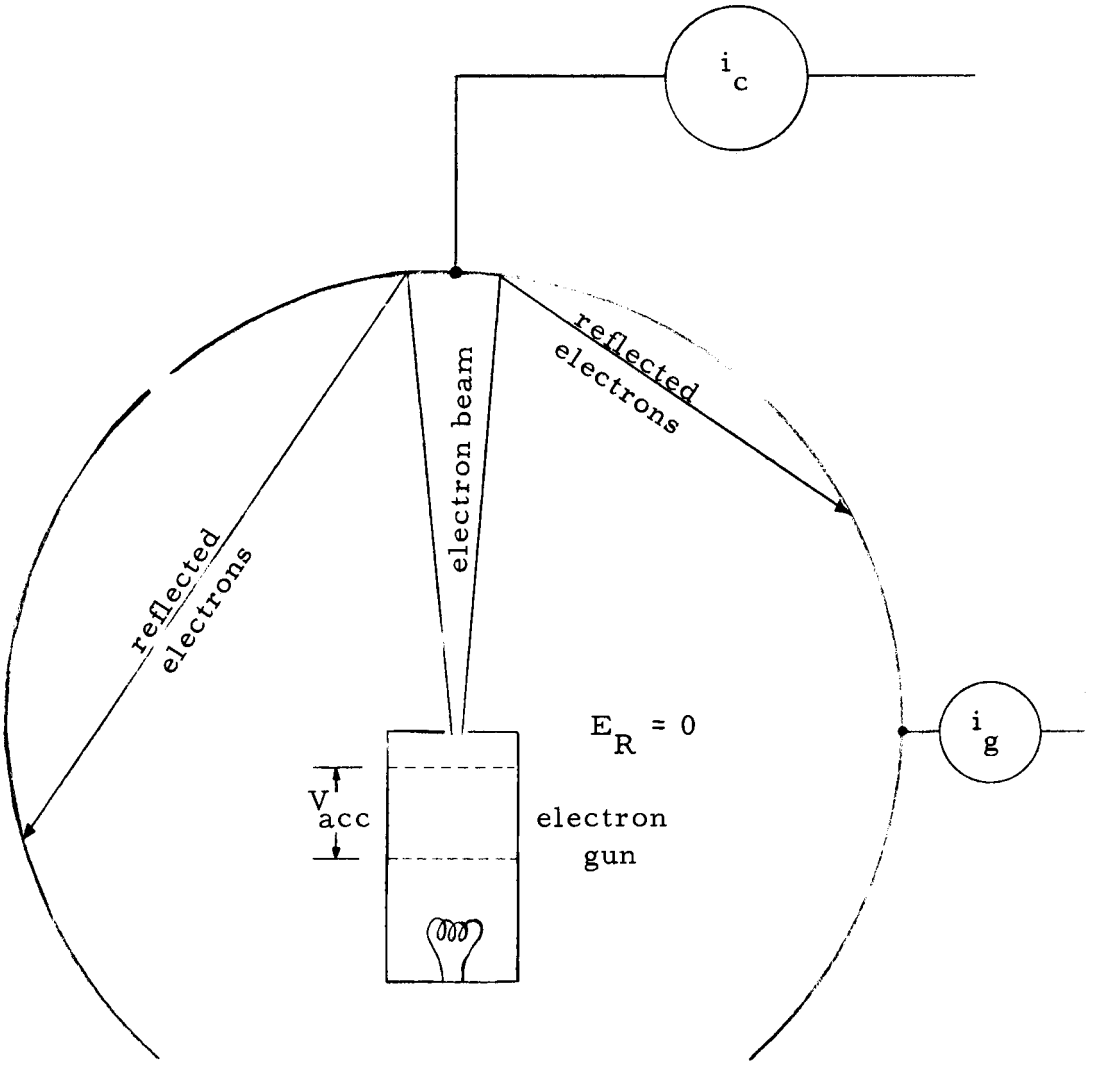


Figure 5. Electron Reflection Experiment.

This quantity is the fractional current due to elastic reflection and secondary emission. A plot of $\delta(\epsilon)$ versus $\epsilon$ may be obtained from repeated measurement of $\delta(\epsilon)$ for different beam energies.

Returning tothe problem of obtaining the electron energy distribution from a point electron source, including the effects of reflection, consider a plot of collector current versus repelling potential, as described in Section 3-2. At the maximum, or cut-off, value of the retarding potential $|Vm|$, electrons impinging on the collector have either been repelled or have lost all their energy, and the surface is presented with electrons of zero energy. For $|V'|$ less than $|Vm|$, the surface is presented with electron energies ranging from 0 eV to $(Vm - V')$ eV; thus, the portion of the $1 - \delta$ curve in effect is that portion in the same range, i. e., from 0 to $(Vm - V')$ eV. Thus

$$i(V') = k_1 \int_{V'}^{V_{max}} V^{\frac{1}{2}}\, T(V - V')g(V)\, dV. \qquad (3\text{-}13)$$

This can be alternatively written as

$$\frac{di}{dV'} = -k_1 g(V')\, T(V'-V')V'^{\frac{1}{2}} + \int_{V'}^{V_{max}} k_1 \frac{\partial}{\partial V'}[T(V-V')]\, V^{\frac{1}{2}} g(V)dV. \qquad (3\text{-}14)$$

The first term is just the expression obtained when reflection is ignored, and the second term represents a correction to the first due to reflection. The magnitude of the correction term depends on

the nature of the functions T and f. If T is independent of the electron energy, the correction is zero, and expression (3-8) results. If T has a relatively small first derivative everywhere, one expects the total reflection correction to be small. Equation (3-13) may be approximated numerically; the method of solution employed in this experiment is presented in the appendix.

Summarizing, if the energy distribution of electrons is measured and doubts concerning the validity of the result because of electron reflection are to be avoided, two experiments must be performed. An experimental curve of i versus repelling potential for the discharge must be obtained as described in Section (3-2); then the function T must be found in the manner described above. The corrected energy distribution may be found from expression (3-13). Finally, it is desirable to have a collector surface with low total secondary emission coefficient for improvement in the signal to noise ratio of the collector current.

# EXPERIMENTAL APPARATUS

This chapter describes in detail each major group of components: the gas handling system, discharge cell, analyzer, electron gun, and external measuring apparatus for both the discharge and electron reflection experiments. A block diagram of the entire apparatus is displayed in Figure 6.

## Gas Handling System

The helium gas used for obtaining the final data was high purity research grade Airco helium in one liter flasks at slightly below atmospheric pressure. A purity report furnished with each flask indicated impurity levels of below four parts per million as determined by mass spectrometer analysis, except for a neon impurity level of ten parts per million. Closed flasks of the gas were sealed on the system A T-joint was included to permit preliminary flushing of the system with tank-grade helium before admitting the pure helium to the system No pure gas was admitted to the system until the pressure in the main chamber had dropped below $10^{-7}$ torr.

Once the seal was broken, the helium passed through a mechanical Nupro "ultrafine" metering valve and stopcock. The mechanical valve, which is simply a needle valve with a precision machined taper, was quite satisfactory for controlling the rate of gas flow into the

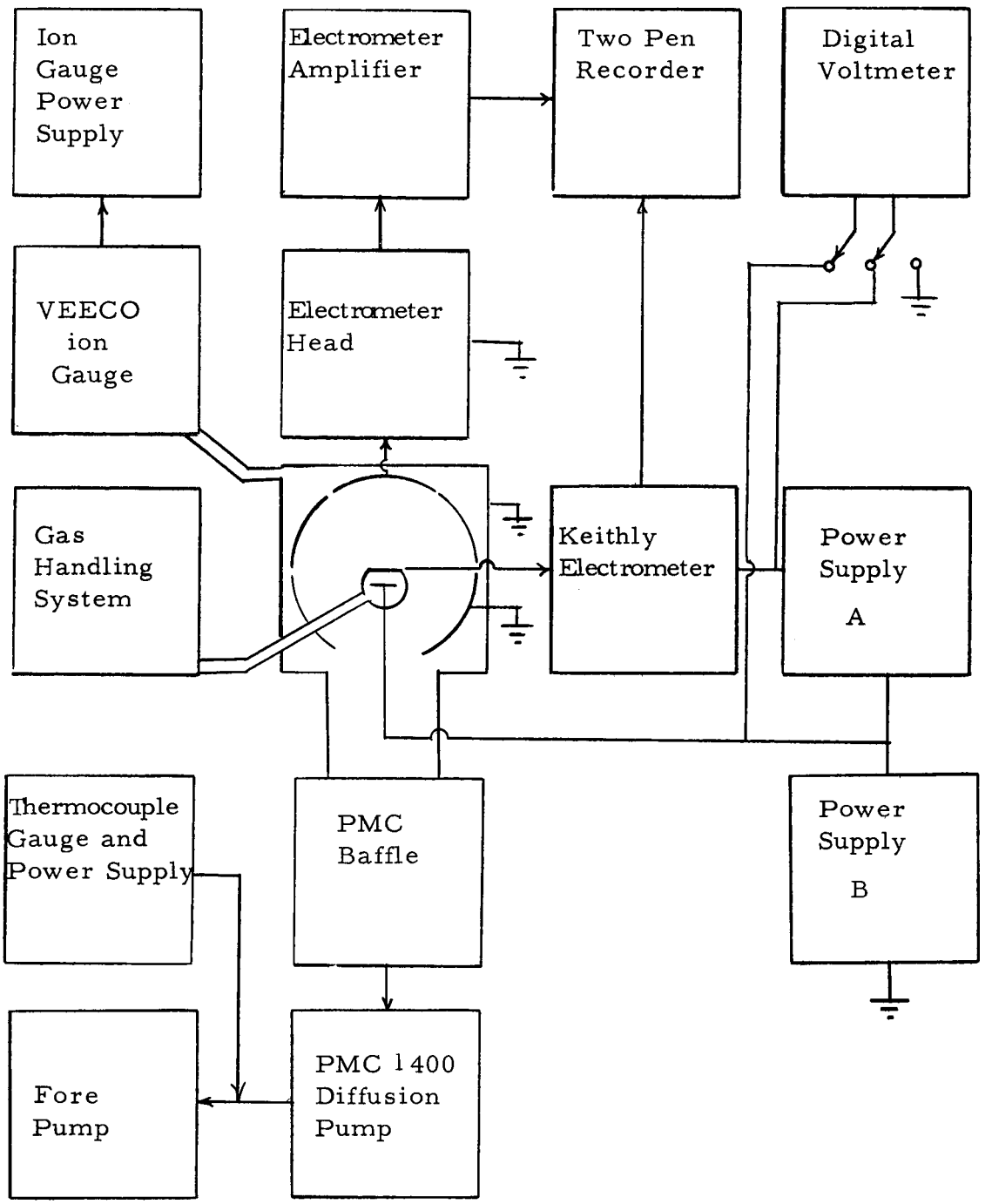


Figure 6. Block Diagram of Apparatus.

cell.

Three traps were provided for further gas purification: a titanium-zirconium trap to remove oxygen (8 , p. 50), a cataphoresis discharge tube for removing the neon impurity, and a liquid nitrogen cold trap to reduce water vapor and oil vapor contamination. The titanium-zirconium trap consisted of a pyrex envelope with two kovar-glass electrodes between which several long shavings of titanium-zirconium alloy were spot welded. Power was supplied to the trap by means of a 1 kw autotransformer until the shavings glowed dull red. The trap was operated continuously throughout the experimental runs.

The cataphoresis tube enclosed two plane electrodes about 2 cm. in diameter separated by a distance of about 15 cm. Approximately 1500 VDC was applied between the electrodes, and a current of about 5 ma. was maintained. The magnitude of the discharge current is not critical, nor is the applied potential, although it has been determined that there exists a correlation between current, electrode spacing, and cataphoretic efficiency; in general, the higher the current and the larger the spacing, the better the cataphoretic efficiency (33). It is difficult to say with any degree of certainty how much neon impurity was removed by cataphoresis, since impurity levels were already at the threshold of mass spectrometer analysis. L. M. Chanin states that for an ultrahigh vacuum system, one observes a decrease of the measured first Townsend coefficient at low $\frac{E}{p}$ as the helium becomes

more pure, until some constant value is achieved (2). It is then assumed that all impurities have been removed. Since the gas handling system was not bakeable, and no low $\frac{E}{p}$ measurements were carried out, it was not possible to detect any appreciable difference in the magnitude of $\alpha$. For this reason, no checks were made throughout most of the experiment. The cataphoresis tube was generally run for several hours before any experimental data were taken, however.

The cold trap was a conventional liquid nitrogen trap, placed in such a way to trap oil vapor from the bypass line and oil and water vapor from the gas line.

The pressure differential $\Delta p$ was measured with an oil manometer filled with octoil - S diffusion pump oil. The manometer was thoroughly outgassed by heating before any experiments were performed. Pressure differences between cell and chamber were read by means of an optical cathetometer located a few meters from the manometer. Since the density of mercury is 13.38 times greater than that of octoil - S, the pressure difference in torr was obtained by dividing the difference in oil column height by 13.38. There is a slight variation in the density of octoil with temperature, but since the room temperature seldom fluctuated by more than a few degrees Celsius, this variation was ignored.

The trapped helium was then introduced to the discharge cell, a small amount escaping through the perforation in the anode into the

analyzing chamber, where it was pumped out by the diffusion pump, a 1400-liter-per-second Consolidated Vacuum Corporation model PMC-1440, which was filled with Dow Corning Silicone DC-704 oil. Backstreaming into the analyzer chamber was greatly reduced by a baffle placed between the pump and chamber. The low vapor pressure of the DC-704 oil, coupled with the high speed of the pump, permitted a pressure of less than $5 \times 10^{-6}$ torr to be maintained in the chamber during an experimental run. The pressure was measured by a Veeco ionization guage located to the side of the chamber and connected to the chamber by means of a short piece of $\frac{3}{4}$-inch pyrex-kovar tubulation.

The system was protected from possible damage due to water cutoff by a "sure-flo" water interlock connected in series with the diffusion pump power source. Damage due to cooking diffusion pump oil was prevented by use of the pressure relay incorporated in the Veeco gauge power supply.

## The Discharge Cell

The discharge cell, shown in Figure 7, was constructed entirely from kovar sealing Dow Corning #7052 glass. A thin disc seal was fastened to the top of the truncated spherical shell. The cell was spherically shaped to reduce the possibility of wall currents. The top of the kovar anode was ground flat to allow electrons escaping at large

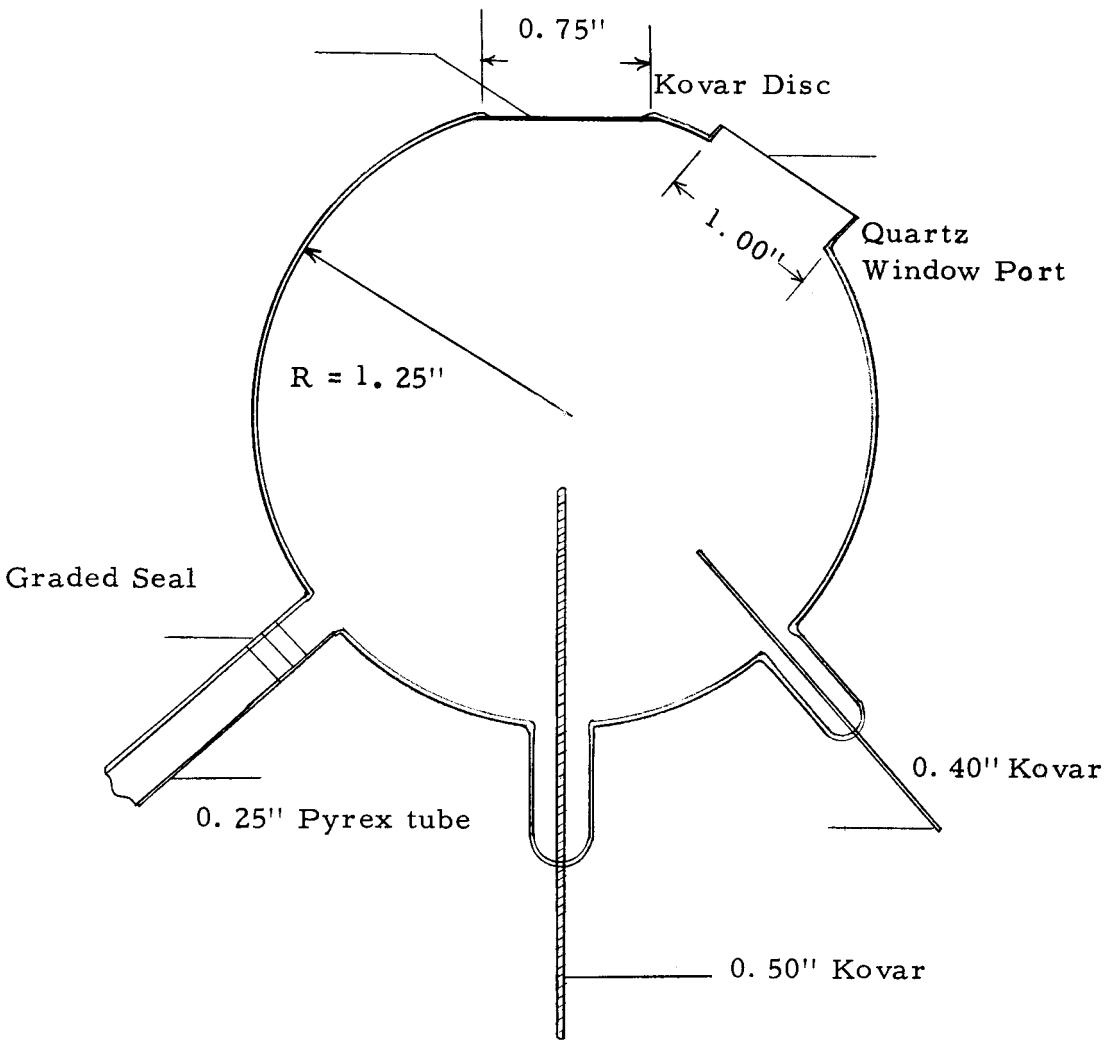


Figure 7. Discharge Cell.

angles to be collected, and to make the anode as thin as possible. The anode was about 0. 2 mm thick after grinding. The anode hole was drilled with a jeweler's drill to a diameter of 0. 1 2 mm. A quartz window port was placed as close to the anode disc as possible, to permit incident light to fall on the cathode at as small an incident angle as possible.

It was discovered early in the experiment that an ordinary metal photocathode would not be adequate as a source of electrons because of insufficient photoemission. A barium-strontium oxide cathode, which has been investigated and found to have a low work function when properly activated (4), was prepared by depositing a thin layer of a $(Ba, Sr)_2CO_3$ suspension in an inert binder on an electropolished nickel disc 0. 75 inches in diameter. The disc was positioned over a heating element and heated to about 600° C. for ten minutes and held at 900° C. for two minutes. During the last two minutes, an electric field was applied between cathode and anode. The high cathode temperature served to convert rapidly the carbonate to an oxide, (Ba, Sr)O, and the application of the field brought about a migration of Ba and Sr ions to the surface, creating a Ba-Sr layer on top of the oxide. The photocurrent from a cathode of this type a few minutes after activation was 300 to 400 times greater than the current from an unactivated cathode.

The discharge cell was supported in the chamber by the gas

feed line. A thin strip of aquadag along the gas line from the anode served as a current lead for the anode. The other end of the aquadag strip was terminated by a clip to which the chamber lead was attached. Prior to mounting and painting on the aquadag strip, the cell was cleaned with trichloroethylene and acetone, then scrubbed thoroughly with "Naconal" laboratory detergent, and finally scrubbed and repeatedly washed in distilled water.

## Electron Gun

The electron gun used in the reflection experiment was based on the simple "immersion" type of design.

A thoriated tungsten ribbon, the central part of which was used as an electron source, was threaded through two holes in a boron nitride cylinder. The directly-heated tungsten filament was used, rather than an indirectly-heated oxide type of thermionic emitter, after it was found that the oxide cathode deteriorated rapidly upon repeated exposure to air and could not be reactivated. The filament assembly was mounted in a cylindrical housing, as shown in Figure 8; and the plane disc at the end of the housing, together with another disc inside, served as the elements of the immersion electron lens. Since the field outside the gun was zero for the reflection experiments, the focal length of the gun was approximately $\frac{-4V}{E}$, where $E$ is the electric field between the elements, and $V$ is the potential at the center of the

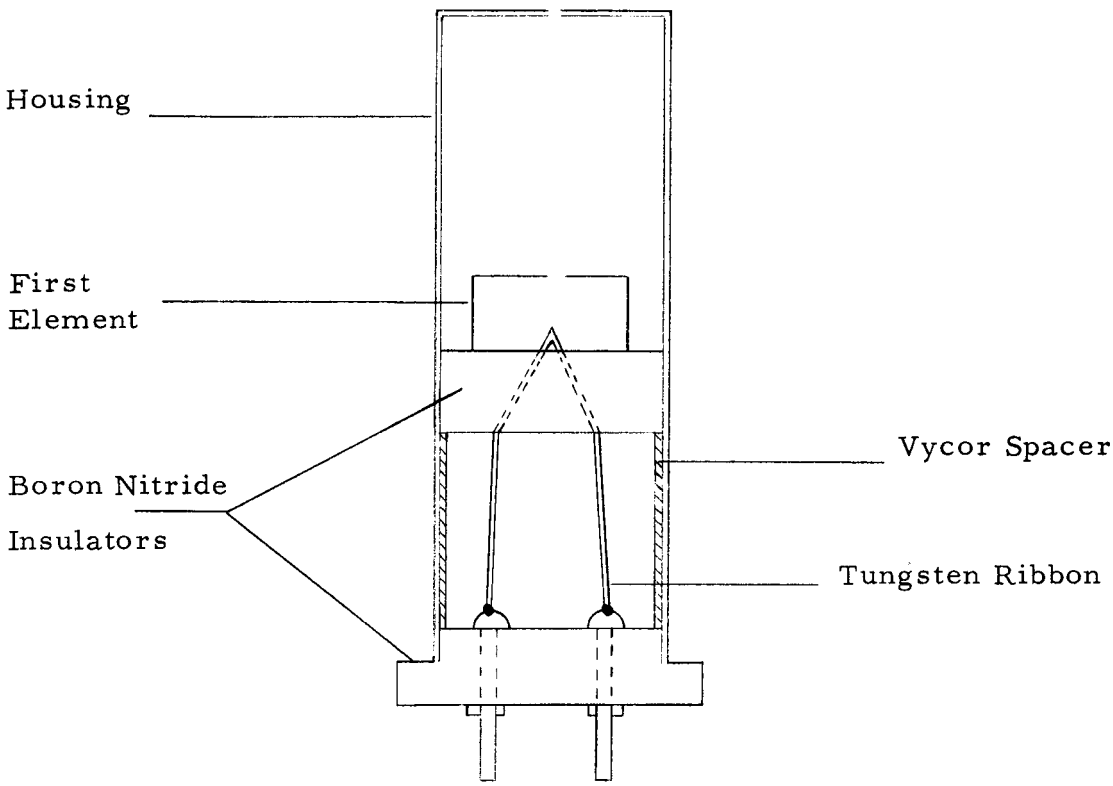


Figure 8. Electron Gun.

final hole (30, p. 96) and is nearly linearly dependent on E because of fringing effects at the aperture (25, p. 205). Thus, the focal length of the gun was nearly constant for a range of accelerating energies from about 1 eV to 100 eV. V could not be determined with sufficient certainty to obtain a reliable value of f. It was required that all the beam current fall incident on the collector only; this condition was indeed satisfied. When the collector was replaced by a smaller disc of the same material, the incident current was the same. Thus, none of the primary current was being collected by the guard shields, and the electron beam was sufficiently well-defined.

It was assumed that the potential drop across the tungsten ribbon was linear, and the potential of the central emitting portion was taken as one-half the applied filament voltage for the purposes of calculating accelerating potentials. The filament potential was 5.5 volts, supplied from a storage battery.

## Analyzer Assembly

The spherical shell which served as collector and guard surface was formed from a pure copper ball float 7.5 inches in diameter. The float was separated along a great circle of the sphere to permit the lower half and upper half of the sphere to be held at different potentials, should such a need arise; the collector portion of the upper sphere was separated so the angle subtended by the collector at the

center of the sphere would be 0.15 ($4\pi$) Steradians. The diameter of the float was uniform to within 0.2 inches, or about 3.0 percent.

The sphere was gold plated, as were all leads, to minimize possible difficulties arising from contact differences of potential. The entire assembly was fastened to an aluminum frame, which supported the sections by means of kovar-glass insulators which were silver-soldered to the sphere sections. The three sections of the sphere were individually adjustable to permit precise centering. The analyzer assembly was vertically aligned visually, with the aid of a cathetometer. It was centered on the anode hole by means of a positioning cross hair temporarily fastened to the upper guard shield.

The inner surface of the sphere was coated with gold black, a porous, filamentary deposit of gold metal, to reduce the total secondary emission coefficient of the collector and guard surfaces. The procedure used for obtaining a gold black surface was roughly in accordance with methods employed elsewhere (12; 6). A 15-mil gold wire was wrapped around the apex of a V formed from 40-mil tungsten wire which was placed in a vacuum chamber 9 cm. from the surface to be coated. With a pressure of $10^{-6}$ torr in the chamber, the tungsten wire was heated until the gold had melted to form a bead on the wire. Hydrogen gas was admitted to the chamber until the pressure was about 2 torr, and the current in the tungsten wire was raised to permit evaporation of the gold. The resulting surface was optically

black and quite fragile from a standpoint of mechanical strength. The nature of this sort of deposit has been investigated by others (29; 31) who have observed that the gold is deposited in tiny crystals about 25 angstroms in diameter. This network of tiny crystals apparently serves to trap incident electrons in the same way a Faraday cup does; i. e., even if reflection occurs, electrons within the mesh are still unable to escape. It was found experimentally that the surface did indeed exhibit a low total secondary emission coefficient; a full description of the experiment and results appears later in this report.

The outer portion of the aluminum support was covered with "Conetic AA" magnetic shielding foil to reduce the horizontal component of the geomagnetic field. Gaussmeter measurements at the discharge cell anode indicated a field strength of about 0. 2 gauss without the foil, and a field strength of less than about 0. 05 gauss (the limit of sensitivity of the instrument) with the foil in place.

A light entry hole 0. 75 inches in diameter was punched in the guard shell and magnetic shielding foil to permit a collimated beam of ultraviolet light to fall incident on the discharge cell window.

## External Electronic Apparatus

The magnitude of the current in the collector circuit was measured with a Cary vibrating reed electrometer. The sensing unit of this device, which is essentially a vibrating metallic reed between the

plates of a capacitor and an A. C. amplifier (28), is housed in a chassis separate from the remaining circuitry and is commonly termed the electrometer "head". This unit was mounted in an inverted position directly on the aluminum lid of the vacuum chamber. A two inch brass rod connected the central signal probe of the electrometer with the lead-out conductor of a stupakof seal, the other end of which was connected to the collector shell by a two inch gold-plated wire. The head was supported by an aluminum cylinder fasted to the chamber lid by short machine screws, which also served as an electrostatic shield for the central current lead. The entire current lead was thus only four inches in length and completely shielded electrostatically (the wire inside the chamber being shielded by the conducting chamber walls). This arrangement proved to be very stable and permitted current measurements near the useful sensitivity limit of the electrometer. While it is stated by the manufacturer that the electrometer is capable of detecting a current as small as $10^{-17}$ amperes, the drift rate of the instrument is about $5 \times 10^{-17}$ amperes, and the short period noise level is of the order of $5 \times 10^{-16}$ amperes. The limit of detection is thus somewhat lower than the lowest level at which reliable quantitative measurements may be made. In this experiment it was found that the useful lower limit was roughly an order of magnitude higher than the threshold of detection.

The current in the discharge circuit was measured with a

Keithly 600A electrometer. The accuracy of this instrument is stated by the manufacturer as being three percent of full scale from 3 amperes to $10^{-10}$ amperes, and four percent of full scale from 3 X $10^{-11}$ amperes to $10^{-13}$ amperes.

The outputs of both electrometers were recorded simultaneously by a Leeds and Northrup two-pen "Speedomax G" recorder. This procedure permitted direct visual correlation between fluctuations in discharge current and collector current, thus affording a convenient display of the data for normalization of the collector current.

All potentials were measured with a Cubic V-45 digital voltmeter, an instrument capable of measuring D. C. potential differences from one millivolt to 1099. 9 volts with an accuracy of $\pm$ 0. 01 percent, or plus or minus one digit, whichever is greater. Calibration of the instrument was periodically checked by means of a Weston standard cell connected directly across the input of the voltmeter *.

Biasing arrangements for the electron reflection and energy distribution experiments are shown schematically in Figures 9 and 10. Power sources A and B were separate sides of a Kepco dual D. C. power supply. This D. C. source is a stable, regulated device, each side of which provides potential differences with less than . 01 percent A. C. ripple.

---

*The high input impedance ($10^7$ ohms) of the voltmeter permitted such direct calibration without harming the standard cell.

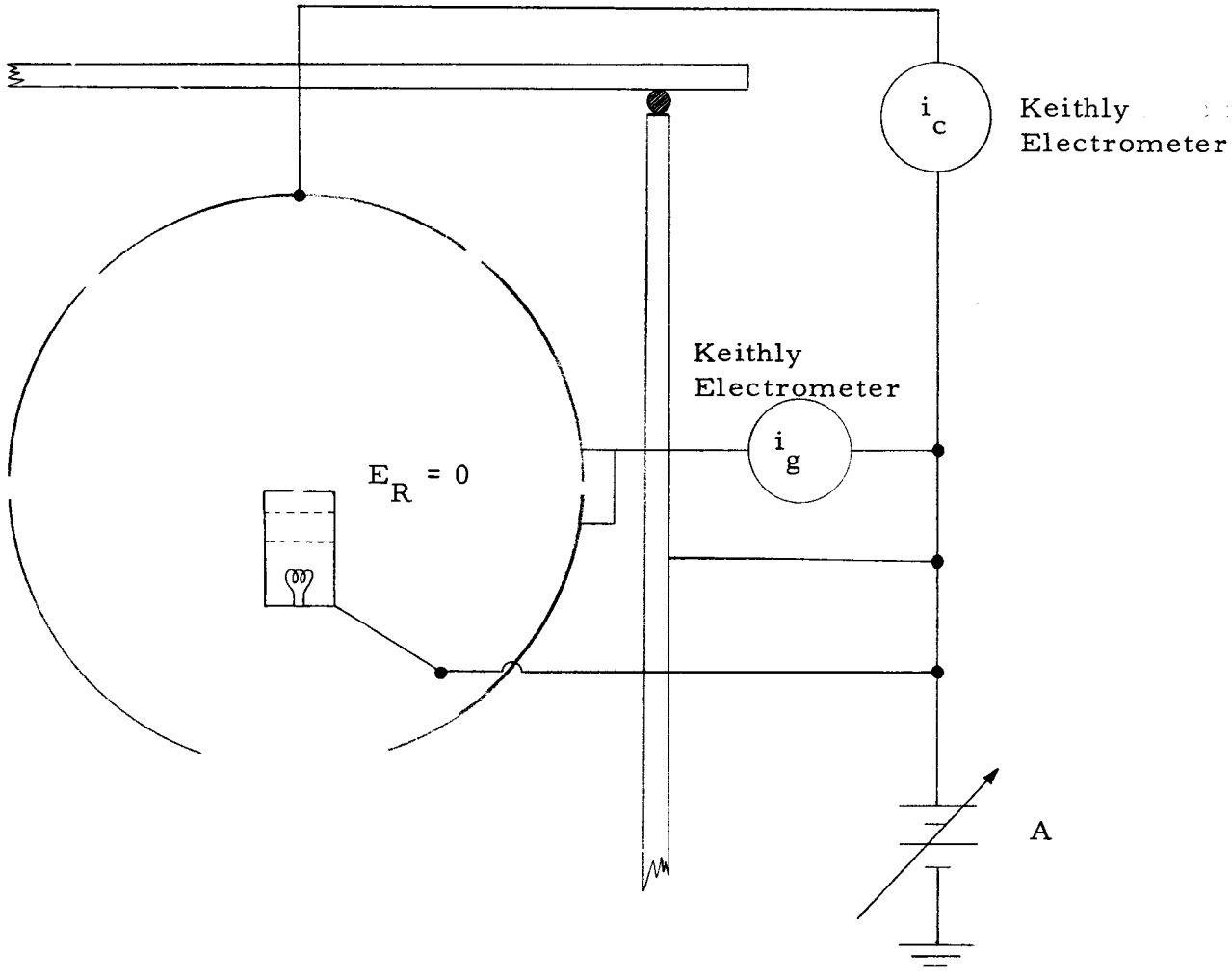


Figure 9. Biasing Arrangement for Electron Reflection Experiment.

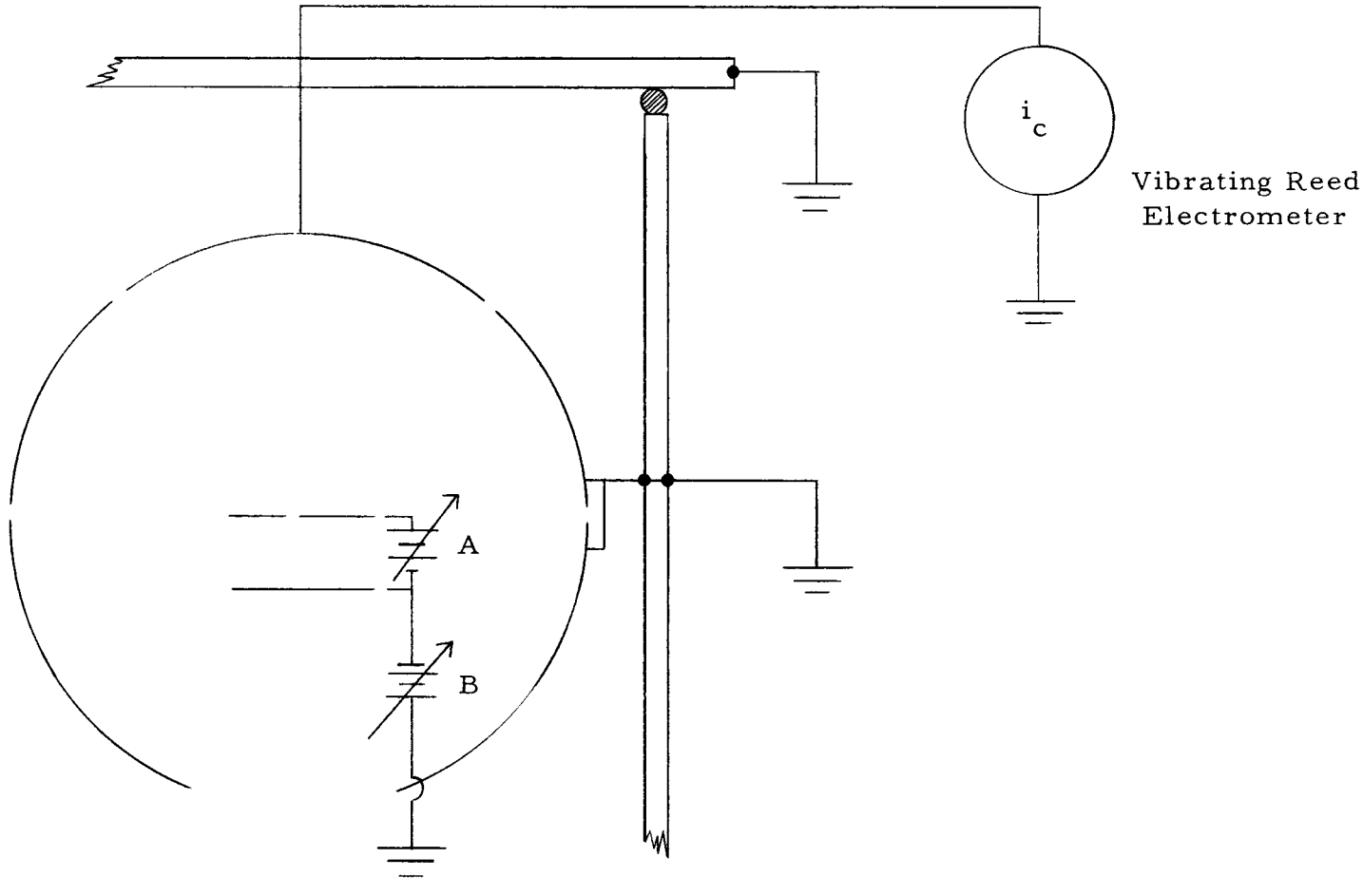


Figure 10. Biasing Arrangement for Energy Distribution Experiment.

# RESULTS AND DISCUSSION

The experimental findings are most logically considered as the results of two separate experiments: the electron reflection determinations and the actual measurements of electron energy distributions in helium discharges.

## Electron Reflection

The first measurements of the total electron secondary emission coefficient were performed using a lampblack deposit as the target surface. Such a coating has long been the surface used for reducing electron reflection and secondary emission. It was the first surface investigated because of the relative simplicity of depositing soot on metal surfaces (an acetylene flame was used to coat the collector and guard shield with soot in this experiment) and because the results of recent measurements of $\delta$ for this coating were available (23). The experimentally determined total secondary emission coefficient for soot is displayed in Figure 11. It is seen that the magnitude of $\delta$ for the soot surface is strongly dependent on preconditioning, and reproducibility is quite poor. The value of $\delta$ at one electron volt ranges between .18 and .24, which is comparable to the value of $\delta \approx .21$ obtained by Marmet and Kerwin. The poor reproducibility, coupled

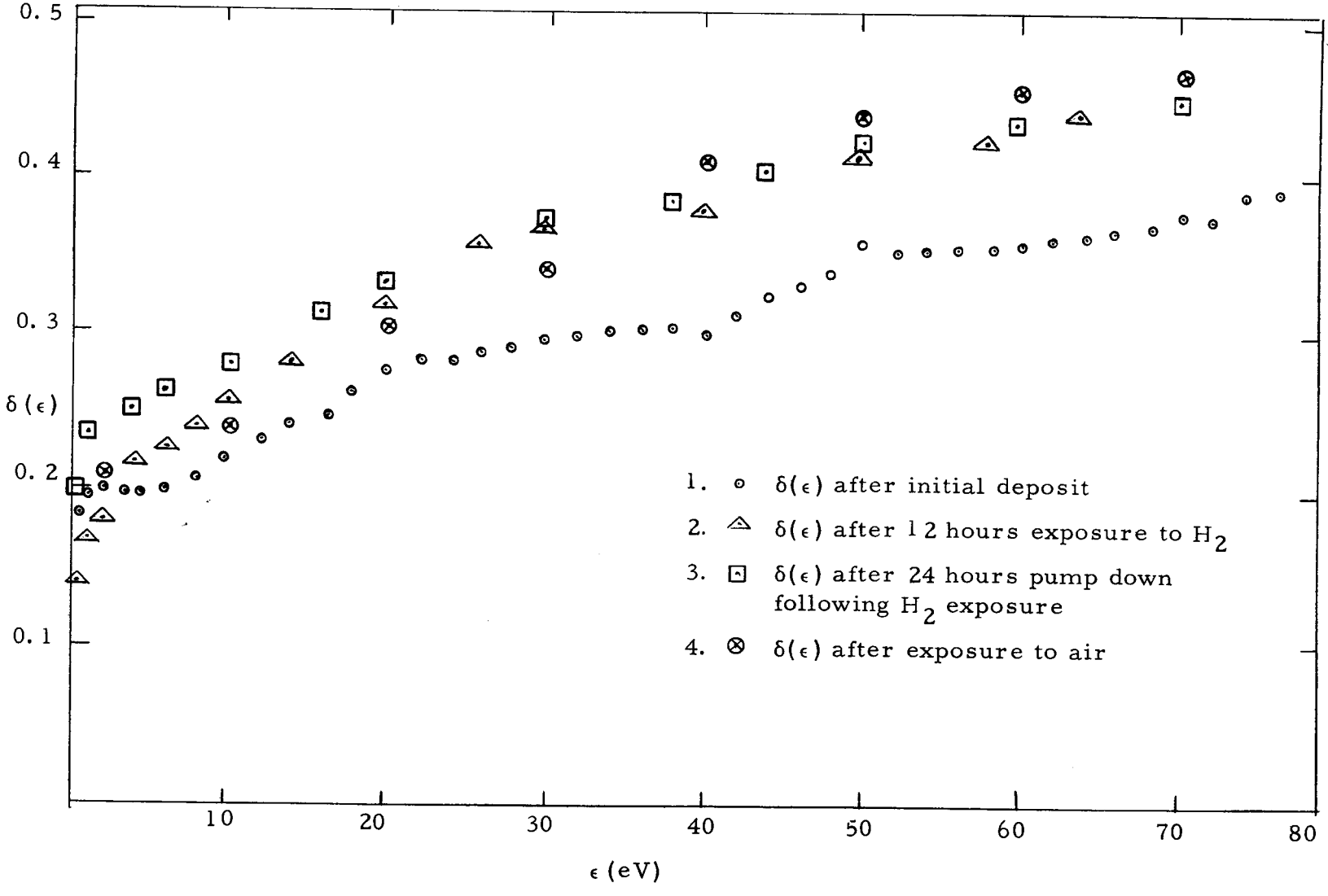


Figure 11. Representative Values of $\delta(\epsilon)$ for Soot Surfaces.

with an observed tendency of the soot surface to outgas*, resulted in abandonment of the lampblack deposit as the surface for use in the energy distribution determinations.

In Figure 12 a comparison of $\delta$ for gold black and polycrystalline gold is presented. Reproducibility of the experimental data for gold black was about five percent for eight different runs. Exposure to various gases failed to alter results appreciably for the black surface. Reproducibility of the curve for polycrystalline gold was very poor, and the curve for this surface is presented only to indicate the drastically reduced total secondary emission coefficient for the gold black.

The characteristic low energy maximum of $\delta$ for gold, which has been observed for other polycrystalline metals (9) is absent or very slight for the gold black surface. A possible explanation of this behavior lies in a consideration of likely mechanisms of electron capture by the metallic black surface. One such mechanism may arise from the porous, filamentary nature of the deposit. This could cause incident electrons to become trapped in the network of fibers, resulting in collection even after several reflections or secondary emissions within the mesh. Another possibility is to view the surface as an

---

*The lowest chamber pressure obtained during any of the experiments on soot surfaces was about $5 \times 10^{-6}$ torr, compared to $10^{-7}$ torr obtained with other surfaces.

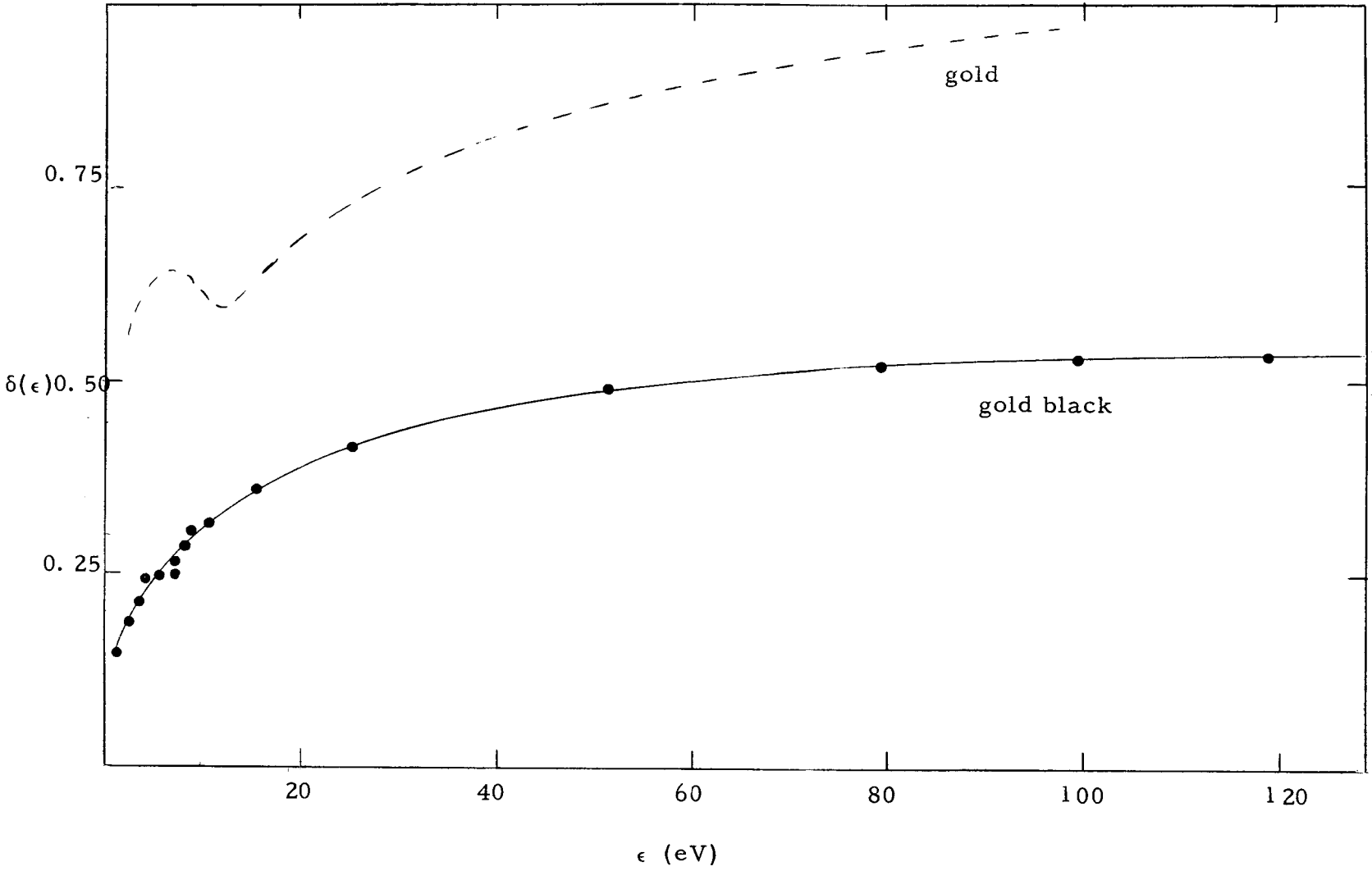


Figure 12. Total Secondary Emission Coefficient for Gold Black and Gold.

array of needle points facing the incident stream of electrons. Incident particles are deflected toward the points, because of the strong local fields associated with sharp points, and are collected after many reflections between adjacent needles. In either case, the mechanism would be quite different from what one might expect for plane surfaces.

There is no adequate theoretical picture describing the phenomenon of electron reflection from surfaces (24, p. 323). Massey and Burhop have stated that the low energy (electron energies below 20 eV) behavior of the total secondary emission coefficient curve is largely due to elastic reflection of electrons, rather than to true secondary emission, but that as electron energies increase, the contribution due to reflection becomes less important. Calculations by MacColl (22) have yielded results which are in rough qualitative agreement with observed data (1) but which give quantitative results which are far too low. Surface cleanliness plays a great role in studies performed on plane single crystal or polycrystalline surfaces. The likelihood of a different mechanism for electron capture due to the physical porosity of gold black seems to reduce the importance of cleanliness in obtaining reliable measurements of $\delta$ for such surfaces. The observed good reproducibility of the data supports this viewpoint.

The energy half-width of the electron beam was measured by applying a retarding potential between the analyzer sphere and electron gun housing. It was found that the electron beam had an energy

half-width of about 0. 3 eV. While this wasjudged adequate for the purpose of this experiment, i. e., to obtain a quantitative estimate of the behavior of the total secondary emission coefficient of gold black, the energy spread was greater than that which can be achieved with more complicated electron gun designs. Possible fine structure details at the low end of the energy spectrum may have been obliterated by the incident electron energy spread. For this reason, conclusions or conjecture dealing with the physical details of electron reflection arising from this experiment are not to be regarded as definitive.

## Energy Distribution of Electrons in Helium

The data obtained directly by experiment are shown graphically for $\frac{E}{p}$ = 200, 150, 100, and 50 in Figures 13, 14, 15, and 16 respectively. These data were obtained in the following way:

1. After appropriate cathode activitation, operation of all traps for several hours, equipment warm-up, etc., gas was admitted to the discharge cell at the desired pressure, usually about 1. 2 torr. The discharge potential was applied to obtain the particular value of $\frac{E}{p}$ under study.
2. The retarding potential was set at some desired level, and the system was allowed to remain in this state for a minute or so to allow for any transient behavior which might be encountered.

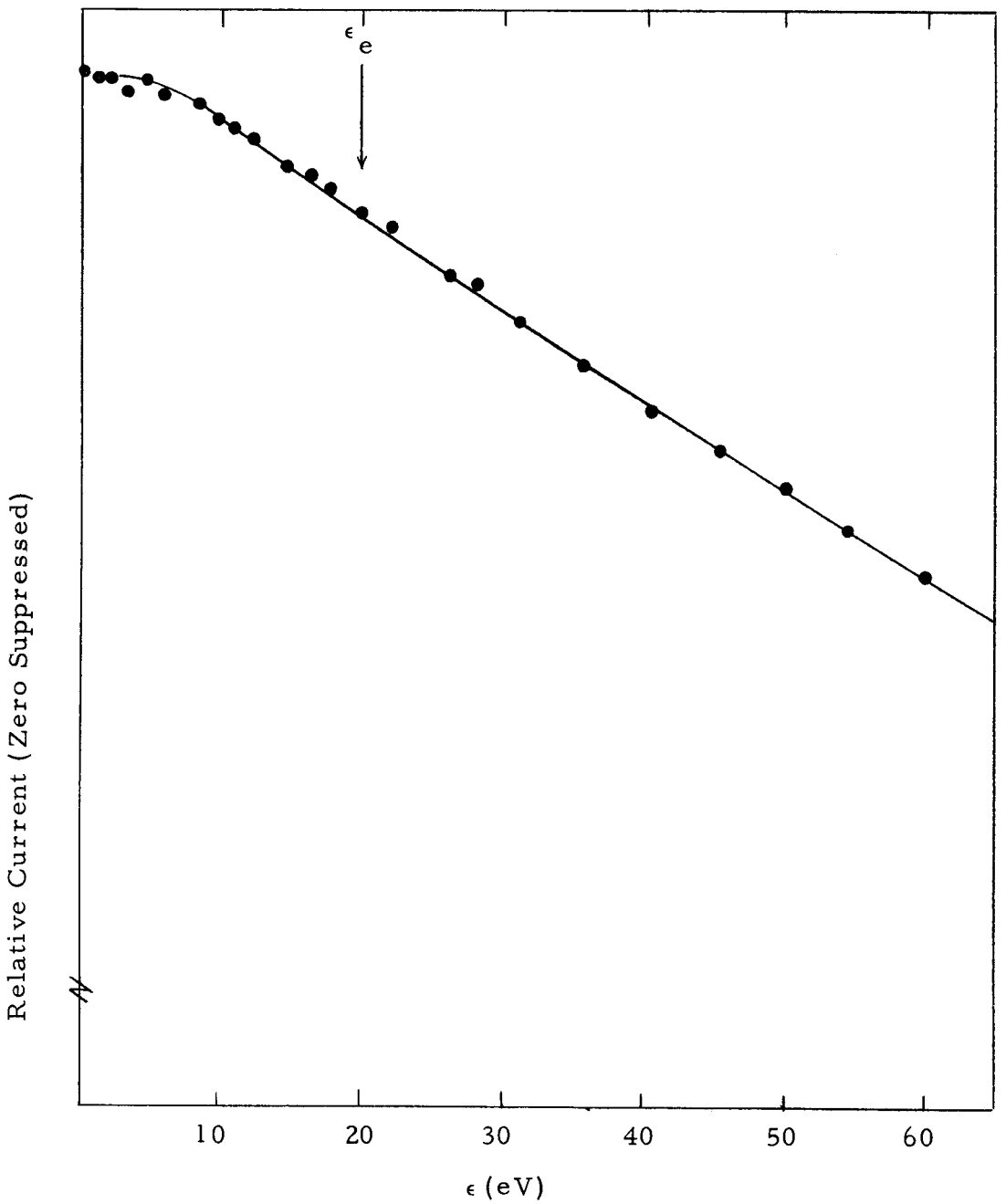


Figure 13. Current vs. Retarding Potential Curve for $\frac{E}{p} = 200$. The True Zero Current Line Lies 2" below the Abscissa Line.

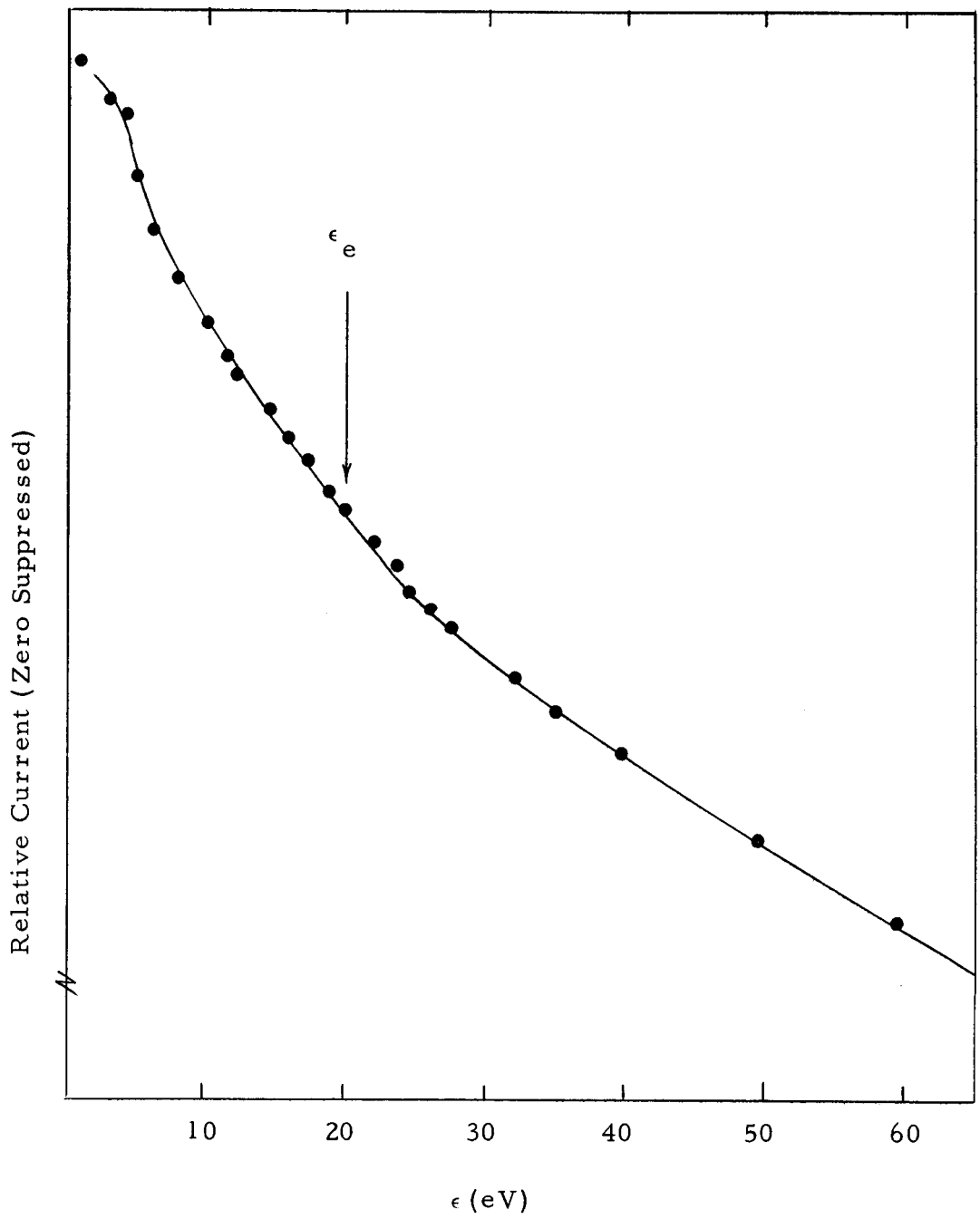


Figure 14. Current vs. Retarding Potential Curve for $\frac{E}{p} = 150$. The True Zero Current Line Lies 2 1/8" below the Abscissa Line.

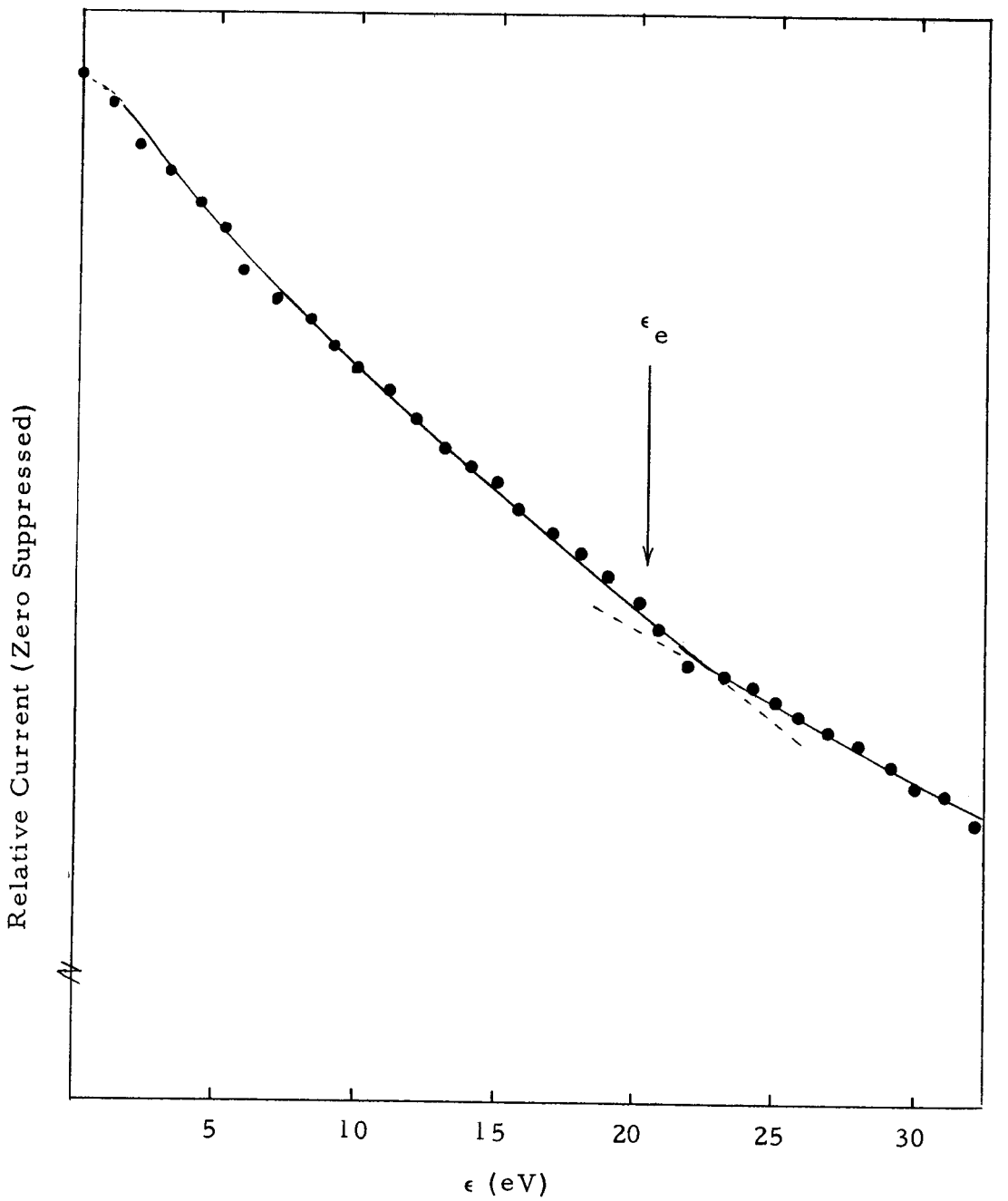


Figure 15. Current vs. Retarding Potential Curve for $\frac{E}{p} = 100$. The True Zero Current Line Lies 1 7/8 " below the Abscissa Line.

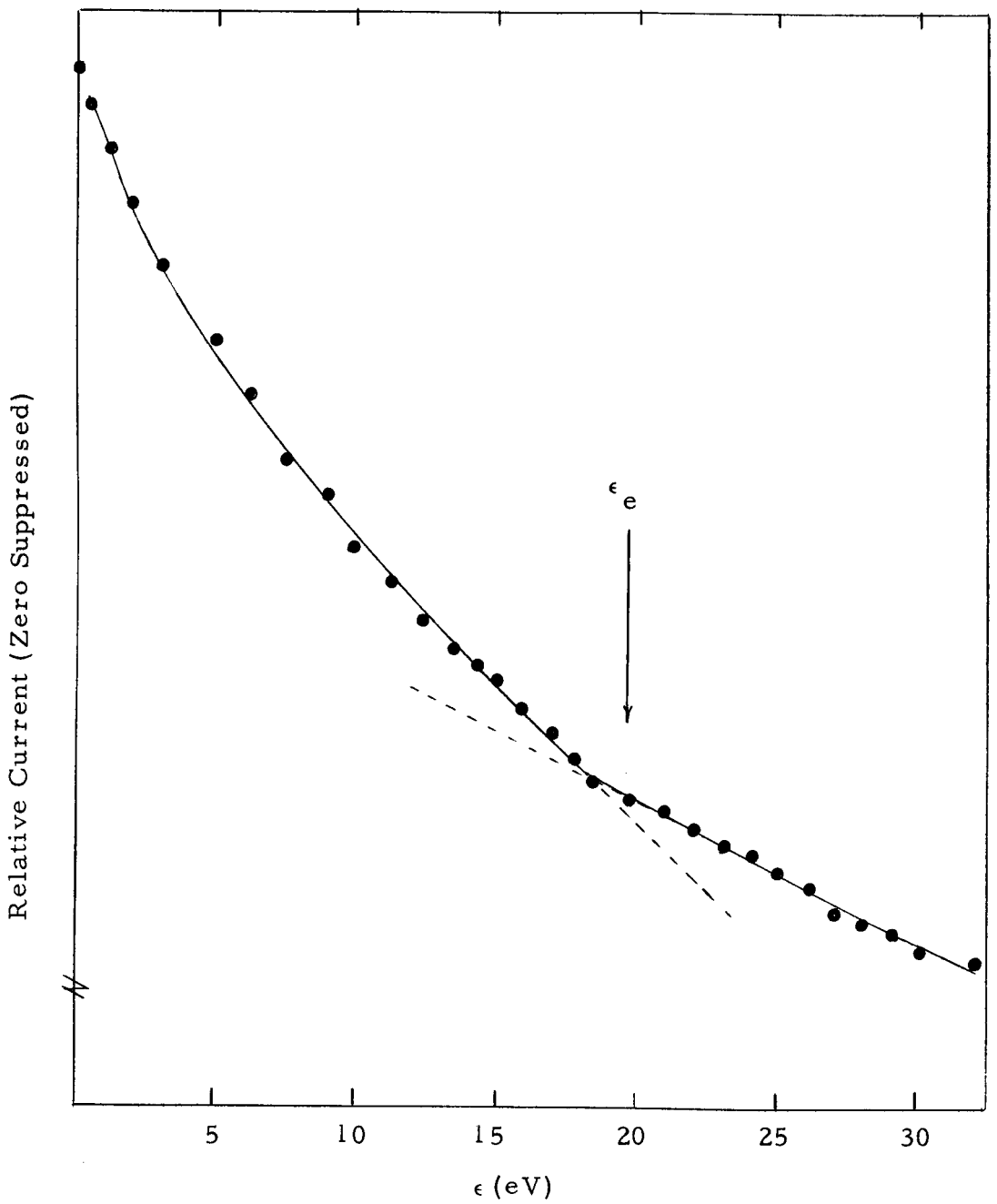


Figure 16. Current vs. Retarding Potential Curve for $\frac{E}{p} = 50$. The True Zero Current Line Lies 1 3/4 " below the Abscissa Line.

3. A charge accumulation versus time plot of collector current was made with ultraviolet light illuminating the photocathode. The discharge current was monitored simultaneously.
4. The light beam was interrupted, and another charge versus time plot was made to obtain the background current due to leakage, random electron emission, etc.
5. Step three was repeated.
6. The net collector current was then the algebraic difference between the average $\frac{dQ}{dt}$ obtained from steps 3 and 5 minus that obtained from step 4.
7. The retarding potential was set at some new level, and the cycle was repeated.

The net average collector current was then divided by the discharge current to normalize for effects of long-time fluctuations in light intensity and cathode efficiency.

A typical raw data plot is shown in Figure 17. The close correlation between fluctuations in the discharge current and the collector current, and the good linearity of the charge versus time data, are strong indications of good system sensitivity and the insignificance of dielectric charging currents. The slope of the curve, $\frac{dQ}{dt}$, yields a current of $2 \times 10^{-14}$ amperes for this particular example. A typical plot of charge accumulation versus time is shown for a value of $\frac{dQ}{dt}$

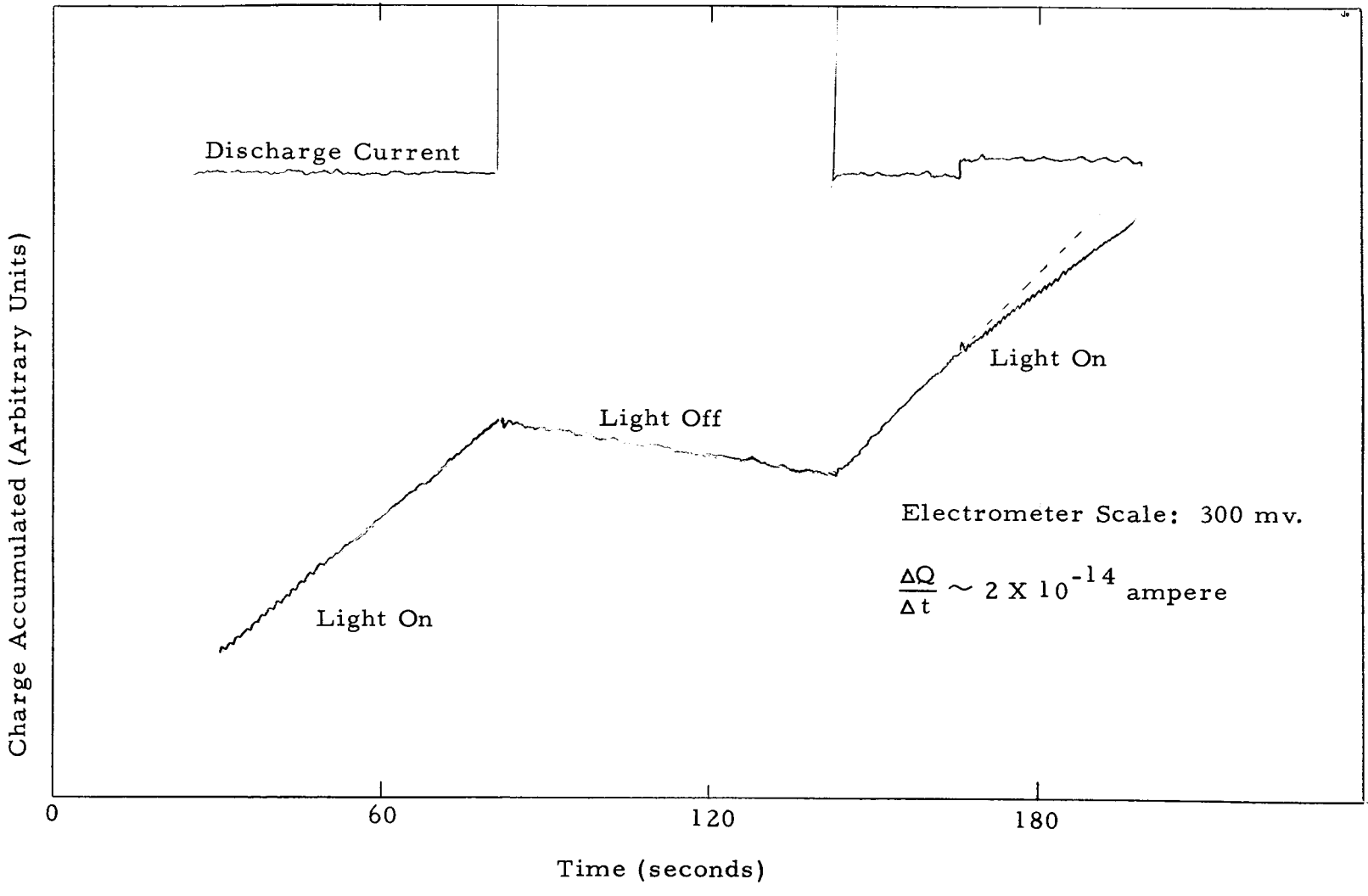


Figure 17. Typical Raw Recorder Data at Relatively High Current Level.

somewhat above the useful sensitivity limit of the electrometer in Figure 18; in this case, the measured current was about $8 \times 10^{-16}$ amperes. The fluctuation about the mean line is rather marked. There is also a tendency toward non-linearity, most likely due to charging of the glass leadout insulators, although this departure is only a few percent. A likely order of magnitude estimate of such charging currents would thus be a few percent of $10^{-16}$ amperes, say $10^{-17}$ amperes.

The question of possible effects due to contact differences of potential was resolved by a simple experiment. The gas was pumped out of the discharge chamber so the pressure in the cell was the same as in the analyzer region, about $10^{-7}$ torr. The incident ultraviolet light then released photoelectrons, which were accelerated by the field between cathode and anode without interaction because of the low gas pressure in the cell. The energy of the least energetic of the electrons arriving at the anode perforation was simply the energy acquired through the potential rise region in the cell. A retarding field experiment was performed to obtain the current versus retarding potential characteristic curve for the photoelectrons. If there were no appreciable contact differences of potential, this curve would be a horizontal straight line, i - constant, until the value $V_{acc}$, the accelerating potential is attained. At this point, the current would start decreasing. At two or so electron volts beyond the retarding potential

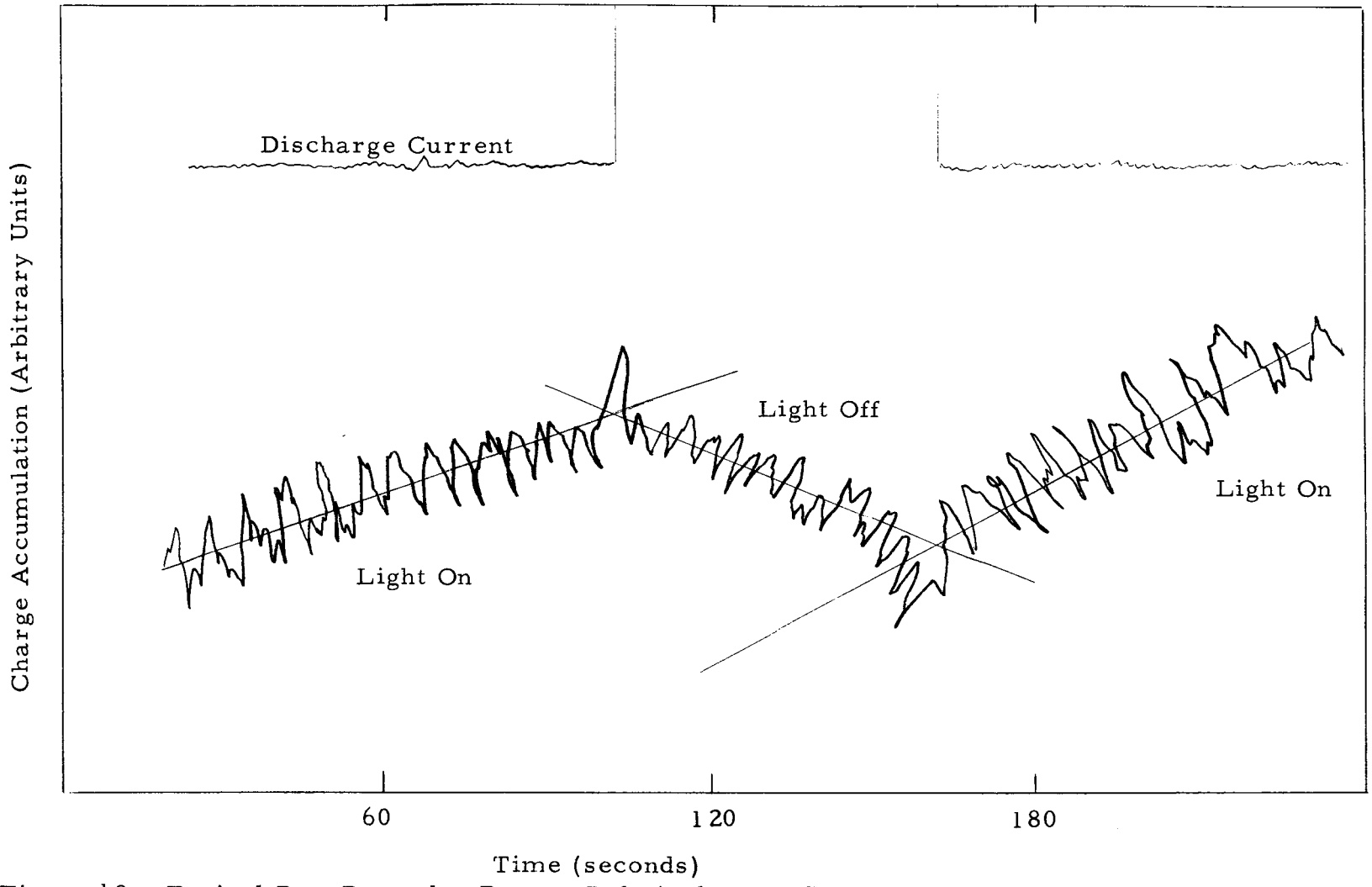


Figure 18. Typical Raw Recorder Data at Relatively Low Current Level.

at the onset of the decrease, the current should have dropped to zero, since the energy spread of photoelectrons is normally only a volt or two.

The result of this experiment is depicted in Figure 19. It is clear that contact differences of potential were somewhat less than one volt because the current versus retarding potential curve appears to begin falling off at the accelerating potential, 66.5 volts.

The curves obtained from a direct plot of the data (corrected for changes in the discharge current) as a function of electron energy were used to obtain values of I(E) at integer values of eV; these values, the retarding potential, and corresponding values of $\delta$ for gold black then served as in-data for the Alwac III-E computer, which was programmed to numerically solve Equation 3-13.

When the mean free path of particles in a gas is of the order of, or larger than, the largest dimension of an opening in a container wall separating two regions of differing pressure, the speed distribution representing the behavior of the particles on the low pressure side of the opening is equal to the product of the speed distribution on the high pressure side of the orifice and the speed, c.

The number of particles per unit volume moving with speeds c, c + dc, is f(c)dc. If the particles move approximately equally in all directions, the fraction $\frac{d\omega}{4\pi}$ are moving into the solid angle $d\omega$. Of these molecules, the number crossing an area dS during a time dt

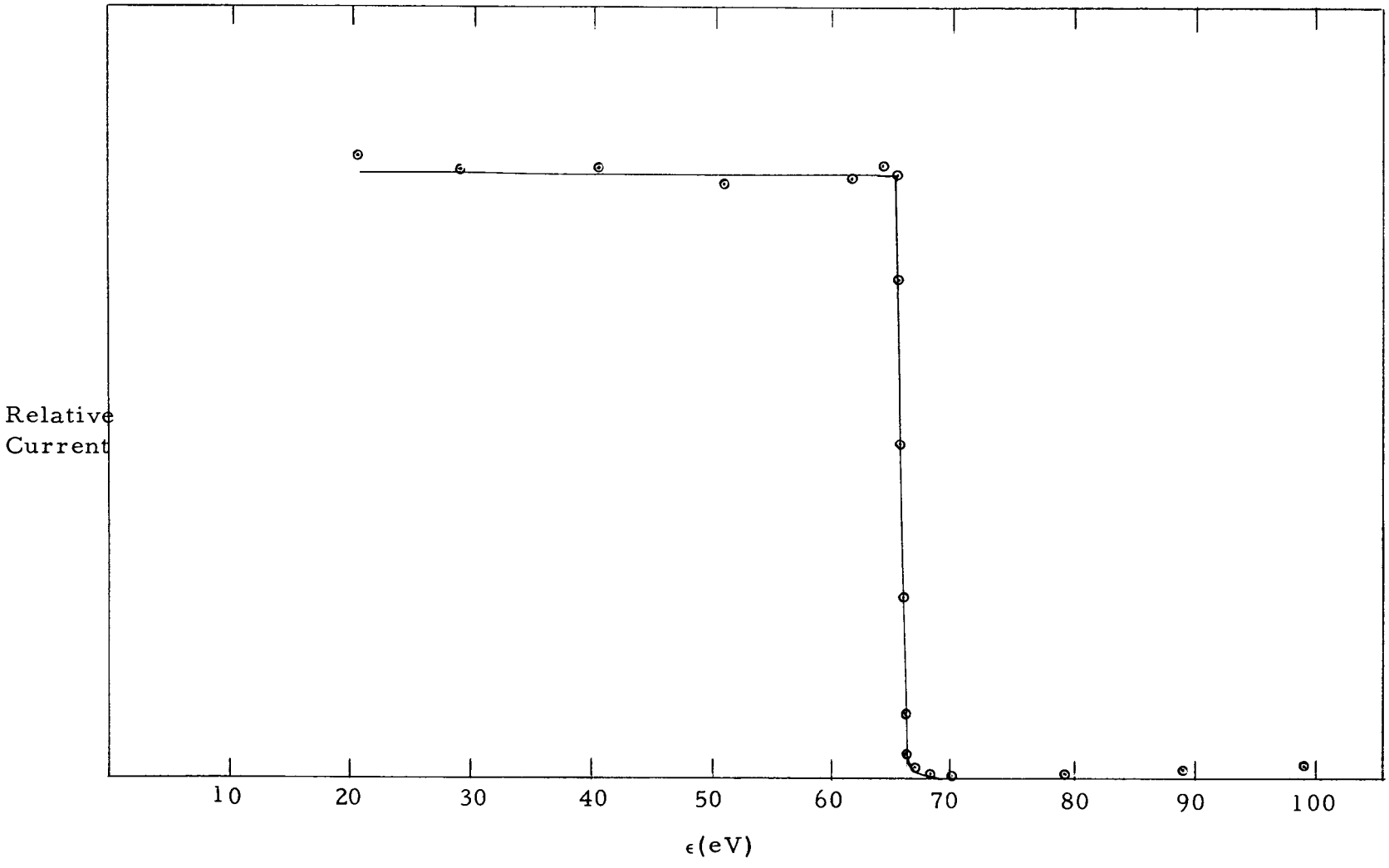


Figure 19. Characteristic Curve for 66.5 eV Photoelectrons.

at an angle $\theta$ with the normal to the surface is the number contained in the cylinder (dct) dS cos $\theta$. The number per unit volume crossing per unit area with speeds c, c + dc into the solid angle $d\omega$ per second is then:

$$\frac{f(c)dc(cdt)\cos\theta\ \frac{d\omega}{4\pi}\ dS}{dS\ dt} \equiv Kcf(c)dc.$$

The appearance of the linear factor c is a result of the assumption of effusive flow*. When the dimension of the opening is much larger than the mean free path of the particles under consideration, the above argument no longer holds. In this experiment, the mean free path of the electrons was always about 0.1 mm, which was very nearly the diameter of the anode perforation. Under these conditions, the flow mechanism has been shown to be more than 98 percent effusive. The assumption of effusive flow is essentially incorporated into expression 3-13, and accounts for the appearance of a factor $V^{\frac{1}{2}}$ in the first term and in the integrand as well.

The final reduced experimental data appear in Figures 20 - 23, together with Heylen and Lewis' theoretical curves for appropriate

---

*Here, effusive flow is taken to mean molecular flow across a boundary because of the effect of the individual, or "peculiar", velocities of the particles only, rather than because of any macroscopic mass flow speed which may characterize the gas as a whole.

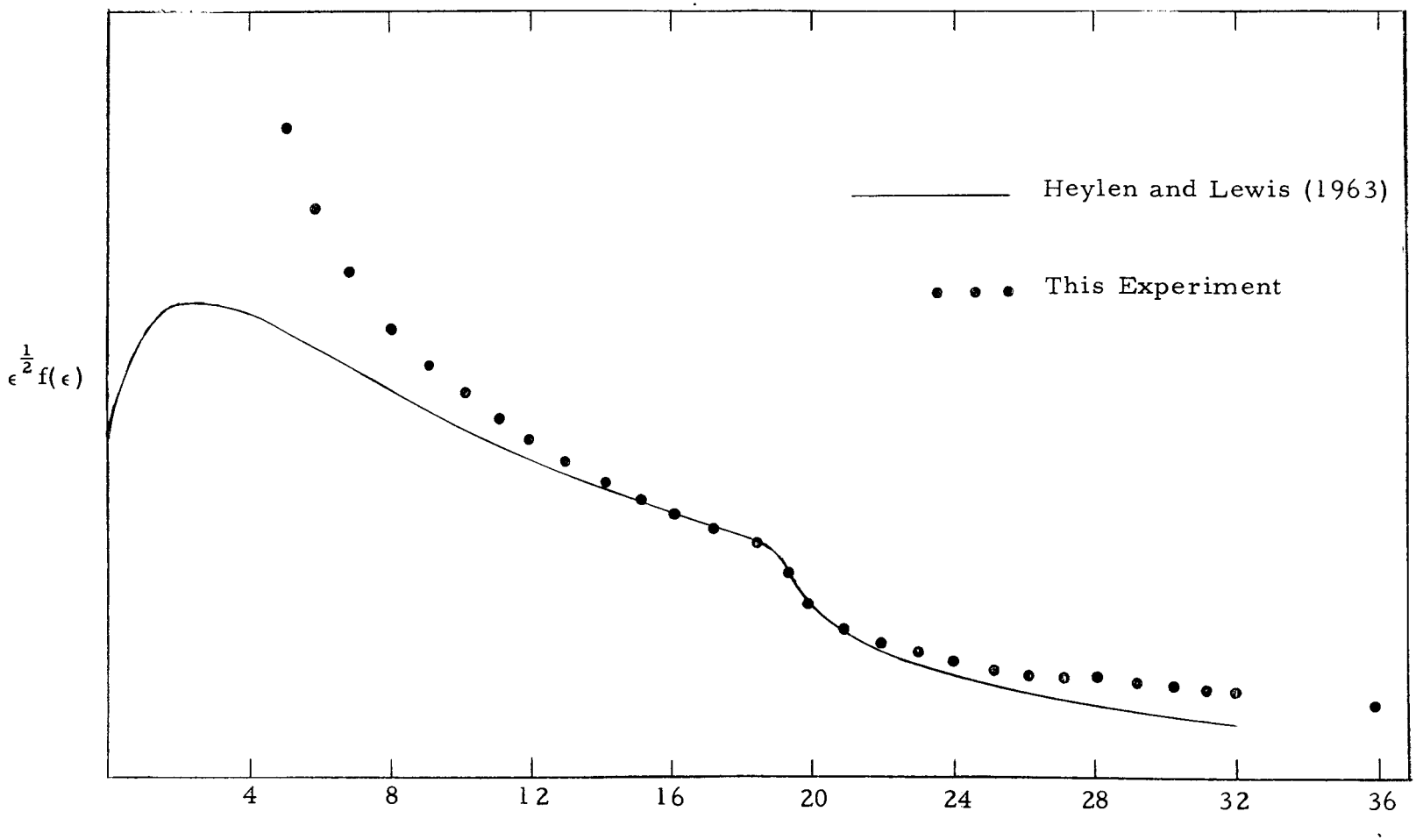


Figure 20. $\epsilon^{\frac{1}{2}} f(\epsilon)$ for $\frac{E}{p} = 50$.

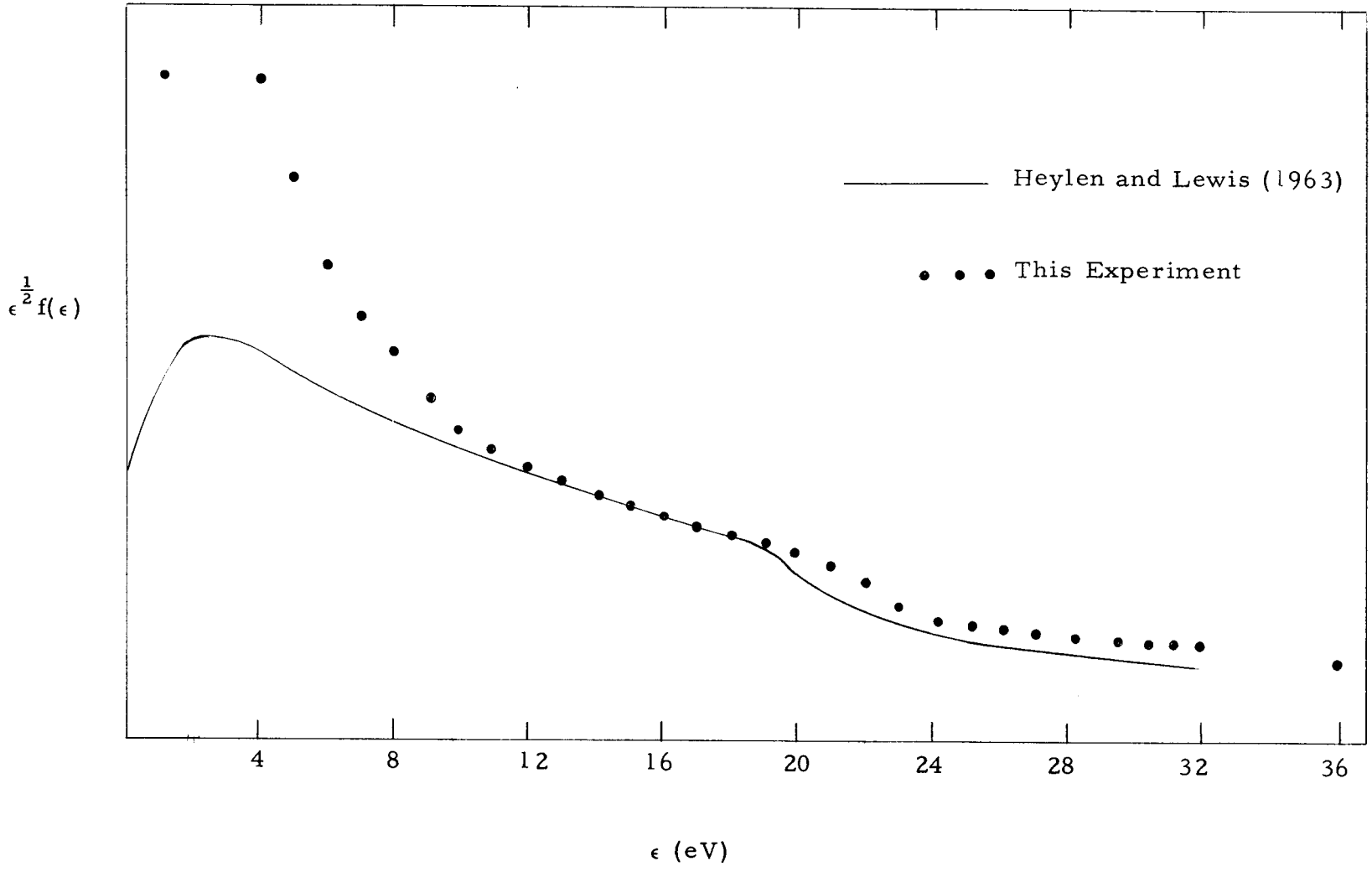


Figure 21. $\epsilon^{\frac{1}{2}} f(\epsilon)$ for $\frac{E}{p} = 100$.

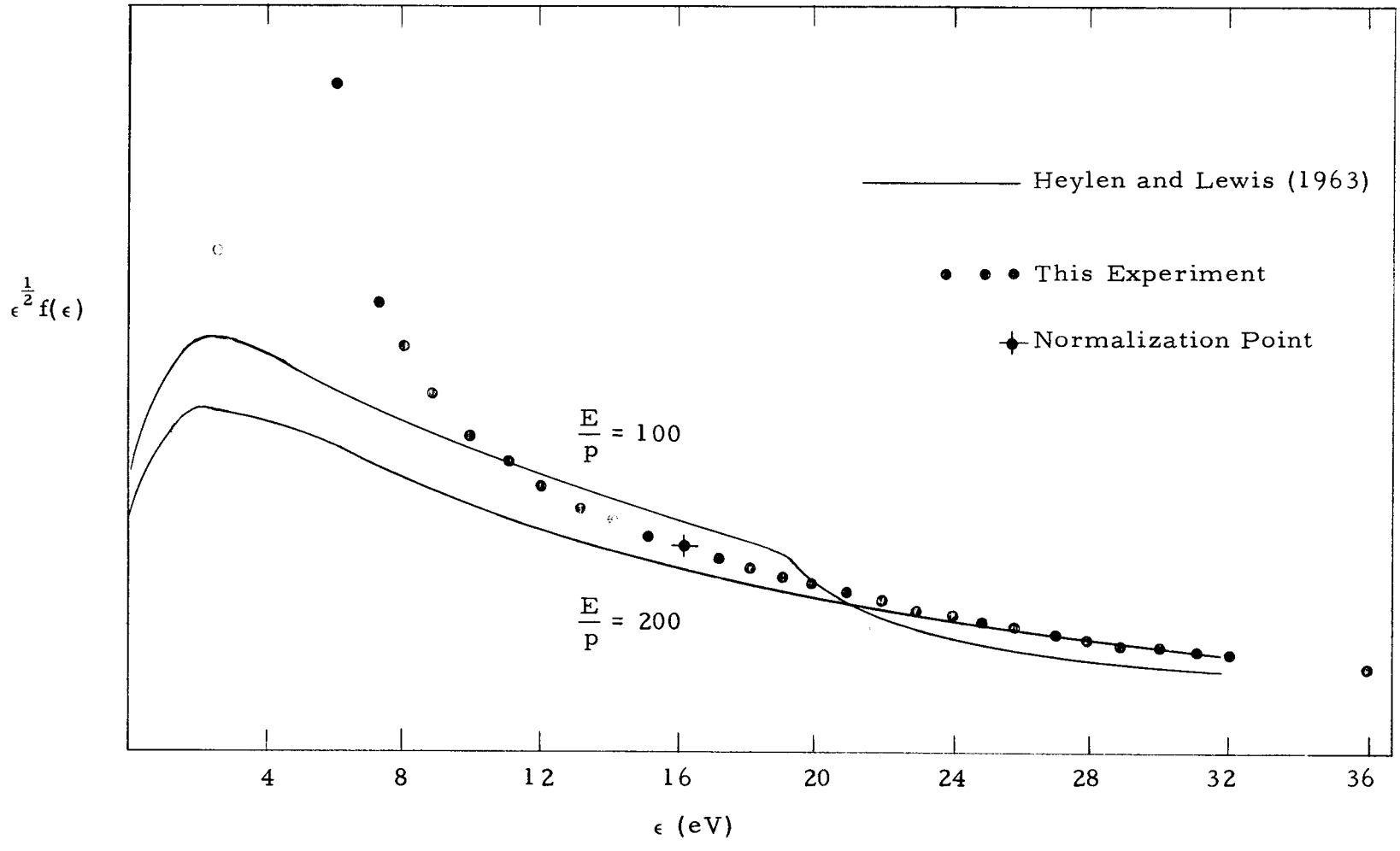


Figure 22. $\epsilon^{\frac{1}{2}} f(\epsilon)$ for $\frac{E}{p} = 150$.

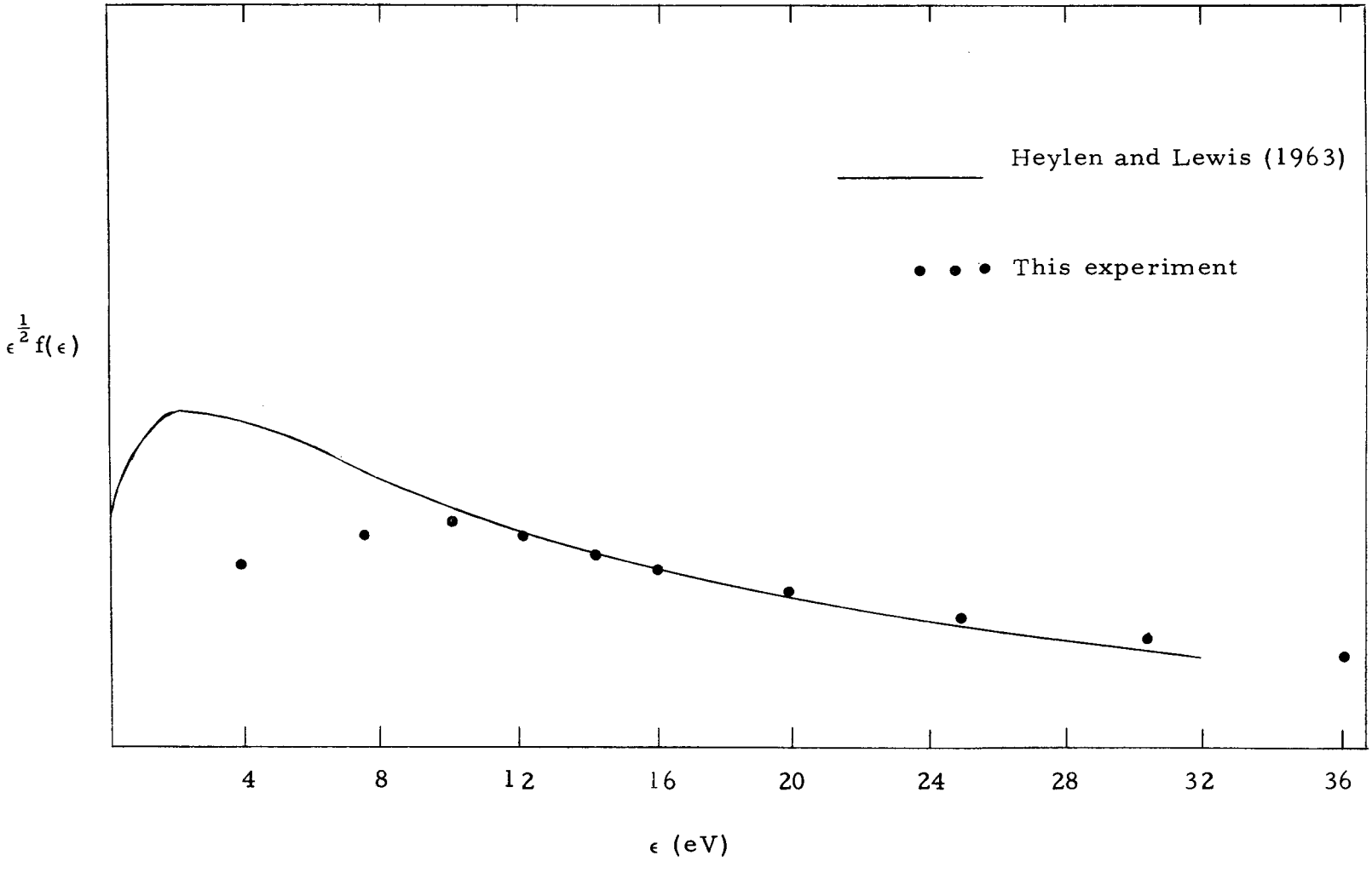


Figure 23. $\epsilon^{\frac{1}{2}} f(\epsilon)$ for $\frac{E}{p} = 200$.

values of $\frac{E}{p}$. Normalization was accomplished by setting the theoretical and experimental values of f(E) numerically equal at $\epsilon$ = 16 eV. It is felt that this method of normalization best compares the nature of the "break" in the curve near the ionization potential of helium. Area normalization was not possible, because only a portion of the total curve was available. The possible use of a truncated area--for example, the area under the curve out to 32 electron volts--was judged to be ambiguous and perhaps less informative than the method of point normalization chosen.

Examination of the comparison between theory and experiment reveals that the energy distribution of electrons for helium exhibits a change in slope near the first excitation potential of helium. The change in the first derivative around the excitation potential becomes less severe with increasing $\frac{E}{p}$; at $\frac{E}{p}$ = 200, there is no apparent change at all.

The position of the maximum along the abscissa seems in agreement with the theory of Lewis and Heylen, save for $\frac{E}{p}$ = 200. Care should be taken to avoid attaching much significance to either the theoretical or the experimental curves at energies much below five electron volts. It has been pointed out in the section concerning the theoretical development that assumptions made by Lewis and Heylen cast some doubt on the validity of the theoretical function at energies below a few electron volts. There is also doubt concerning the

apparent experimental result because of several factors, one of which is the behavior of the collision cross section of helium at low electron energies. Helium, like all noble gases, exhibits a maximum in the total electron momentum transfer $\theta$ at about 1 eV (10). While the effect is not as pronounced as it is in many of the other noble gases, the cross section is still larger at 1 eV than at 7 eV. This enhanced cross section necessarily implies a greater number of collisions for very low energy electrons in the region immediately exterior to the discharge cell, where gas atoms from the cell would have a higher concentration than anywhere else in the analyzer chamber. The collisions exterior to the discharge occur under the influence of a non-uniform electric field, Townsend conditions no longer prevail, and subsequent alteration of the energy distribution seems likely. The complexity of the problem, since the gas concentration gradient immediately outside is not known, precludes any theoretical attempts to correct the experimental data. The effect of the residual magnetic field after shielding becomes increasingly important as the electronic energy decreases, as does the effect of possible electric field inhomogeneities or the possible release of low energy photoelectrons from the anode surface because of the action of reflected ultraviolet light. It is not feasible to account for the many alterations that may occur in the measured distribution at low energies because of the phenomena mentioned above, so the low energy results must be viewed with

caution. In the study of higher energy electrons, of course, the lower energy electrons are retarded and never reach the collector.

The maximum uncertainty implicit in the process of finding curves by differentiating a succession of data points which exhibit a fluctuation about some mean functional curve is simply $\frac{\Delta y}{\Delta x}$, where $\Delta y$ is the total deviation from the mean of the ordinate between successive points, and $\Delta x$ is the abscissa increment successive points (14, p. 83). For portions of the data curve where slopes are steep, this maximum uncertainty can become quite large. It has been shown above (Equation 3-14) that the data curve $i(\epsilon)$ is related to the energy distribution by the first derivative $\frac{di}{d\epsilon}$ and a correction term. Because the first derivative is involved, and the maximum of the distribution function occurs essentially at the same value of the abscissa as the steepest portion of the data curve, further uncertainty as to the absolute height of the maximum is present. This and the features mentioned in the previous paragraph limit the quantitative conclusions concerning the energy distributions obtained in this experiment.

The data were also cast into the form of distribution functions by simple differentiation (Equation 3-8) and the results compared with the results obtained by a consideration of electron reflection. It was found that at energies above 5 eV, the correction was slight, resulting in a largest difference at 32 eV between corrected and uncorrected curves of about four or five percent for $\frac{E}{p} = 50$, the corrected

distribution indicating slightly more high energy electrons than the uncorrected curve. Consequently, the data for $\frac{E}{p}$ = 100, 150 and 200 were reduced assuming reflection to be unimportant. Quantitative comparisons at the low energy end of the curve are not very meaningful because of uncertainty in both the total secondary emission coefficient and the data curves in this region. However, the maximum for the corrected curve was slightly lower than for the uncorrected data. Thus, the main conclusion to be derived from the reflection correction is that for well-behaved total secondary emission coefficients, the reflection effect is not as important as might be expected, despite statements by others which have indicated otherwise (27, p. 32). This explains previous successes with the retarding field method (11, p.176-231) and invalidates, in part, some of the criticisms leveled at this type of experiment.

Finally, the measurements were not extended to lower values of $\frac{E}{p}$ than $\frac{E}{p}$ = 50 because:

1. Measurements by Chanin and Rork indicate that for low $\frac{E}{p}$, electrons may not reach equilibrium with the electric field at the pressure of about 1 torr used in this experiment (2). Since the distribution being measured is ideally an equilibrium distribution function, the results of measurements for chamber pressures of the order of 1 torr are necessarily ambiguous.

2. The effect of trace impurities becomes more marked at low $\frac{E}{p}$ ( 2 ). Since the system was not bakeable, such trace impurities were probably present in the helium.

3. Collector current magnitudes become smaller at low $\frac{E}{p}$ and approach the sensitivity limit of the apparatus because of decreased discharge currents. Also, there are relatively more low energy electrons present than for higher $\frac{E}{p}$, which increases the uncertainties involved in interpreting results, for reasons discussed previously.

In view of previous comments, several suggestions may be made concerning the course of future investigations using the method described herein. A system capable of withstanding bakeout temperatures would help eliminate any doubts concerning gas purity, and would permit use of clean collecting surfaces coated with extremely low reflectance materials such as the clean platinum black used by R. J. Zollweg (38). Use of such a surface would virtually eliminate any need for a reflection correction.

The single perforation in the cell anode can be replaced with many smaller perforations in a very thin foil mounted in a small center section of the anode; this would serve to increase the signal current and ensure validity of the assumption of effusive flow. Finally, an improved cell should be made in such a way that quick external adjustment of the anode-cathode spacing is possible, so measurements

over a wide range of $\frac{E}{p}$ for various anode-cathode separations may be made for several noble gases besides helium as well as for clean helium at low $\frac{E}{p}$.

# SUMMARY

This investigation of the nature of the electron energy distribution in a helium discharge utilized a spherical retarding field analyzer remote from the region of the discharge itself to obtain electron current versus retarding potential curves. These data yielded distributions which were compared to the theoretical predictions of Heylen and Lewis (3). The following conclusions may be made:

1. Some features of the distribution of electronic energies in a Townsend discharge in helium have been directly determined by experiment. This work represents the first such direct determination.
2. Experimental results are in qualitative agreement with the theoretical predictions of Heylen and Lewis at intermediate values of $\frac{E}{p}$ for helium.
3. There is a large quantitative discrepancy between the theoretical distribution and experiment at low electron energies. This discrepancy becomes smaller with increasing energy and is only a few percent at electron energies above 10 eV, if normalization is appropriately chosen.
4. Conclusions concerning the experimental data at the low energy end of the spectrum are limited by physical effects unique to the collection of low energy electrons by the

apparatus.

5. When a substance with a well-behaved total secondary emission coefficient, such as gold black, is used to coat all collecting surfaces, the effect of correcting experimental results to include electron reflection is to slightly decrease the apparent difference between the probable number of electrons at low energies and the probable number at high (i. e., above 25 eV) energies. The average slope of the apparent distribution function is thus decreased. The total correction amounts to only a few percent.

# BIBLIOGRAPHY


1. Bruining, H. and J. H. deBoer. Secondary electron emission. Physica 5:17-30. 1938.

2. Chanin, Lorne M. and G. D. Rork. Experimental determinations of the first Townsend ionization coefficient in helium. Physical Review, ser 2, 133:A1005-A1009. 1964.

3. Chapman, Sydney and T. G. Cowling. The mathematical theory of non-uniform gases. 2d ed. Cambridge, Cambridge University Press, 1960. 431 p.

4. Devore, H. G. and J. W. Dewdney. Photoconductivity and photoelectric emission of barium oxide. Physical Review 83:805-511. 1951.

5. Dreicer, H. Electron velocity distributions in a partially ionized gas. Physical Review 117:343-354. 1960.

6. Drummond, A. J., The Eppley Laboratory, Inc. Worcester, Massachusetts. Private communication. Nov. 5, 1963.

7. Druyvesteyn, M. J. De invloed der Energieverliezen bij elastische Botsingen in de Theorie der Electronendiffusie. Physica 10:61-70. 1930.

8. Evenson, Kenneth Melvin. Atomic nitrogen recombination studied by electron paramagnetic resonance. Ph. D. thesis. Corvallis, Oregon State University, 1964. 129 numb. leaves.

9. Farnsworth, H. E. Bombardment of metal surfaces by slow moving electrons. Physical Review 20:358-374. 1922.

10. Frost, L. S. and A. V. Phelps. Momentum-transfer cross sections for slow electrons in He, Ar, Kr and Xe from transport coefficients. Physical Review, ser A, 136:1538-1545. 1964.

11. Good, R. H., Jr. and Erwin W. Müeller. Field emission In: Encyclopedia of physics, vol. 21. Berlin, Springer-Verlag, 1956. p. 176-231.

12. Harris, L., R. T. McGinnies and B. M. Siegel. The preparation and properties of gold blacks. Journal of the Optical Society of America 38:582-589. 1948.

13. Heylen, A. E. D. and T. J. Lewis. Electron energy distributions and transport coefficients for the rare gases. Proceedings of the Royal Society of London, ser A, 271:531-550. 1963.

14. Hildebrant, Introduction to Numerical Analysis. New York, McGraw Hill, 1956. 511 p.

15. Holstein, T. Energy distribution of electrons in high frequency gas discharges. Physical Review 70:67-84. 1946.

16. Huang, Kerson. Statistical mechanics. New York, John Wiley and Sons, 1963. 470 p.

17. Johnson, E. O. and L. Malter. A floating double probe method for measurement in gas discharges. Physical Review 80:58-68. 1950.

18. Kahn, I. H., J. P. Hobson and R. A. Armstrong. Reflection and diffraction of slow electrons from single crystals of tungsten. Physical Review 129:1513. 1963.

19. Langer, Rudolph E. On the connection formulas and the solutions of the wave equation. Physical Review 51:669-676. 1937.

20. Loeb, Leonard B. Pasic processes of gaseous electronics. Berkeley, University of California Press, 1955. 1012 p.

21. Lukirsky, P. Über weiche Röntgenstrahlen. Zeitschrift für Physik 22:351-367. 1924.

22. MacColl, L. A. Numerical calculations of reflection of electrons by metals. Physical Review 56:699-702. 1939.

23. Marmet, Paul and Larkin Kerwin. An improved electrostatic electron selector. Canadian Journal of Physics 38:787-796. 1960.

24. Massey, H. S. W. and E. H. S. Burhop. Electronic and ionic impact phenomena. Oxford, Oxford University Press, 1952. 669 p.

25. Meyers, L. M. Electron optics, theoretical and practical. New York, D. Van Nostrand, 1939. 618 p.

26. Morse, P. M., W. P. Allis and E. S. Lamar. Velocity distributions for elastically colliding electrons. Physical Review 48: 412-419. 1935.

27. Nottingham, Wayne B. Thermionic Emission. In: Encyclopedia of physics, vol. 21. Berlin, Springer-Verlag, 1956. p. 1-175.

28. Palevsky, Swank and Grenchik. Design of dynamic condenser electrometers. Review of Scientific Instruments 18:298-314. 1947.

29. Pfund, A. H. Optical properties of metallic and crystalline powders. Journal of the Optical Society of America 23:375-378. 1933.

30. Pierce, J. R. Theory and design of electron beams. 2d ed. New York, D. Van Nostrand, 1954. 222 p.

31. Roess, L. C. and E. N. Daws. The design and construction of rapid-response thermocouples for use as radiation detectors in infra-red spectrographs. Review of Scientific Instruments 16:164-172. 1945.

32. Simpson, J. A. Design of retarding field energy analyzers. Review of Scientific Instruments 32:1283-93. 1961.

33. Schmeltekopf, A. M. Ph. D. thesis. Austin, University of Texas, 1962. 161 numb. leaves.

34. Smit, J. A. Berechnung der Geschwindigkeitsverteilung der Elektronen bei Gasentladungen in Helium. Physica 3: 543-560. 1936.

35. Smythe, William R. Static and dynamic electricity. New York, McGraw-Hill, 1939. 560 p.

36. Soboleva, N. A. The accuracy of the spherical collector method. Rodiotekhnika i Electronika 3:339-344. 1958.

37. Townsend, J. S. and H. T. Tizard. Motion of electrons in gases. Proceedings of the Royal Society of London, ser A, 88:336-347. 1913.

38. Zollweg, R. J. Electron reflection from cesium - coated polycrystallin metals at low primary energy. Journal of Applied Physics, 34: 2590-2598. 1963.

# APPENDIX

# APPENDIX

## Numerical Solution of Equation (3-13)

The form of the equation to be solved is

$$I(x) = \int_x^a T(t - x)\, F(t)\, dt, \tag{7-1}$$

$$\therefore \frac{I(x)}{a - x} = \frac{1}{a - x} \int_x^a T(t - x)\, F(t)\, dt.$$

Hence,

$$\lim_{x \to a} \frac{I(x)}{a-x} = -I'(a) = T(o)F(a) = F(a). \tag{7-2}$$

The integral may be approximated by a sum. Let $x_{i-k}$ and $h$ be defined by

$$x_i - x_k \equiv x_{i-k} ;$$

$$x_j - x_{j-1} \equiv h . \qquad \text{(equal intervals)}$$

Then $$I(x_k) = \sum_{i=k}^{m} T(x_i - x_k)F(x_i)\, \lambda_{i-k} h$$

$$= \sum_{i=k}^{m} \lambda_{i-k} T(x_{i-k})F(x_i)h .$$

Let $$\lambda_i T(x_i) = a_i ,$$

$$\frac{1}{a_o} F(x_i) = y_i ,$$

$$\frac{I(x_i)}{a_o h} = b_i .$$

Hence

$$a_o y_k + \sum_{i=k+1}^{m} a_{i-k} y_i = b_k \tag{7-3}$$

and, from Equation (7-2),

$$y_m = \frac{1}{a_o} F(a) = - \frac{I'(a)}{a_o} . \tag{7-4}$$

It follows that

$$a_o y_{m-1} + a_1 y_m = b_{m-1}$$

$$a_o y_{m-2} + a_1 y_{m-1} + a_2 y_m = b_{m-2}$$

$$\vdots \qquad \vdots \qquad \vdots \qquad \vdots$$

$$a_o y_{m-k'} + \sum_{i=1}^{k} a_i y_{(m-k')+i} = b_{m-k'} .$$

The last equation in this system of equations is ($k' = m$)

$$a_o y_o + \sum_{i=1}^{m} a_i y_i = b_o . \tag{7-5}$$

Thus we have a system of equations with $y_m$ given by (7-4) with known coefficients b, and we can solve for the y's, if the coefficients a are known. Using the trapezoidal rule as an integral approximation,

the original equation to be solved is approximated by sums of products of the a's with the y's, for equally spaced intervals weighted in sequence by 1, 2, 2, , 2, 1. Hence

$$a_i = 2T_i, \text{ except for the final } a_i \text{ in any equation,}$$

$$a_o = T_o = 1,$$

and the general equation of the system of equations becomes for h = 1,

$$y_{m-k} + 2 \sum_{i=1}^{k-1} T_i y_{(m-k)+i} + T_k y_m = b_{m-k},$$

$$\therefore \quad y_{m-k} + 2 \sum_{i=1}^{k-1} T_i y_{(m-k)+i} + T_k y_m = \frac{I_{m-k}}{T_o},$$

where the notation $T_i = T(x_i)$ is used and primes are dropped.

The system of equations to be solved now becomes

$$y_m = -\frac{I'(a)}{T_o} = -I'(a)$$

$$y_{m-1} + T_1 y_m = I_{m-1}$$

$$y_{m-2} + 2T_1 y_{m-1} + T_2 y_m = I_{m-2}$$

$$\vdots \qquad \vdots \qquad \vdots \qquad \vdots$$

$$y_{m-k} + 2 \sum_{i=1}^{k-1} T_i y_{(m-k)+1} + T_k y_m = I_{m-k}$$

$$\vdots \qquad \vdots \qquad \vdots \qquad \vdots$$

$$y_o + 2 \sum_{i=1}^{m-1} T_i y_i + T_m y_m = I_o.$$

The T's and I's are known experimentally. $I'(a)$ can be found from a graphical display of the data; thus, successive values of $y$ may be determined. This completes the solution of the problem.